https://doi.org/10.5194/egusphere-2023-884
Preprint. Discussion started: 19 June 2023
© Author(s) 2023. CC BY 4.0 License.

# Snowmelt-mediated isotopic homogenization of shallow till soil

Filip Muhic[1], Pertti Ala–Aho[1], Matthias Sprenger[2], Björn Klöve[1], Hannu Marttila[1]

[1]Water, Energy and Environmental Engineering Research Unit, University of Oulu, Oulu, Finland
[2]Earth and Environmental Sciences at the Lawrence Berkeley National Laboratory, Berkeley, USA

*Correspondence to*: Filip Muhic (filip.muhic@oulu.fi)

**Abstract.** The hydrological cycle of sub-arctic areas is dominated by the snowmelt event. Understanding the mechanisms that control water fluxes during high-volume infiltration events in sub-arctic till soils is needed to assess how future changes in the timing and magnitude of snowmelt can affect soil water storage dynamics. We conducted a tracer experiment with deuterated water to irrigate a plot on a forested hilltop in Lapland, tracked water fluxes of different mobility and monitored how the later snowmelt modifies the labelled soil water storage. We used lysimeters and destructive soil coring for soil water sampling, and monitored and sampled the groundwater. Surface water flow during the tracer experiment was largely controlled by fill-and-spill mechanism. We found that labelled water remained in deeper soil layers over the winter, but the snowmelt event gradually displaced all deuterated water and fully homogenized all water fluxes at the soil-vegetation interface. The conditions required for the full displacement of the old soil water occur only during snowmelt with a persistently high groundwater table. We propose a conceptual model where infiltration into the soil, and eventual soil water replenishment, occurs in three stages. First, unsaturated macropore flow is initiated via surface microtopography and is directed towards the groundwater storage. The second stage is characterized by groundwater level rise through the macropore network, and subsequent pore water saturation and horizontal connectivity of macropores. Shallow subsurface lateral fluxes develop in more permeable shallow soil layers. In the third stage, which materializes during a long period of a high groundwater table and high hydrological connectivity within the soil, the soil water is replenished via enhanced matrix flow and pore-water exchange with the macropore network.

## 1 Introduction

Soil water storage plays a vital role in sustaining the water cycle and regulating eco-hydrological processes at the soil-vegetation-atmosphere continuum (Sprenger et al., 2016). As biogeochemical fluxes and contaminant transport are controlled by the propagation of precipitation through the landscape, water fluxes that pass through the soil are essential for soil functions (Ma et al., 2017). Soil water storage acts as a link between precipitation and groundwater recharge, while soil moisture stored in the unsaturated (vadose) zone provides the water for plant transpiration (Brooks et al., 2015). Soil moisture storage within the vadose zone is often controlled by highly spatially and temporally variable mixing and transport processes, which are difficult to disentangle (Kampf et al., 2015; Penna et al., 2009; Vereecken et al., 2015). Observed soil

https://doi.org/10.5194/egusphere-2023-884
Preprint. Discussion started: 19 June 2023
© Author(s) 2023. CC BY 4.0 License.

water patterns are often difficult to reproduce through modelling approaches, so a better conceptualization of soil water mixing is needed (Beven and Germann, 2013).

Studies that utilize stable isotopes of water to track water storages and fluxes in the vadose zone are becoming more frequent, as stable isotopes of water have provided new insights into the soil water mixing and transport processes and the interaction between water fluxes that occupy or move through soil pores of different sizes (Good et al., 2015; McDonnell, 2014; Brooks et al., 2010). The mixing dynamics of soil matrix water, usually moving slowly via matrix flow, and macropore water, infiltrating at a much higher velocity to deeper soil layers, influence infiltration patterns, soil moisture redistribution in unsaturated soil and the amount of water available to plants during the growing season (Sprenger and Allen, 2020). It is well established that dominant flow pathways through the soil are strongly influenced by the macropore flow (Klaus et al., 2013), particularly during the infiltration events with high intensity (McDonnell, 1990; Weiler, 2005), in the soils that experience seasonal soil freezing (Hayashi, 2013) and highly structured soils (Flury et al., 1994).

Current studies on soil water mixing based on isotope data are geographically biased towards temperate climates (Tetzlaff et al., 2015), and more high quality data sets from other climate regions are needed. A better understanding of subsurface water pathways is especially important in snow dominated northern areas, where both current and predicted warming rates are highest (Hassol, 2004; Post et al., 2009). The higher latitudes are particularly sensitive to climate change through increased land surface temperatures (Klein Tank et al., 2013), altered snow cover duration and amount (Groisman et al., 1994; Pulliainen et al., 2020; Stiegler et al., 2016), modifications of the freeze/thaw cycles (Hatami and Nazemi, 2022; Henry, 2008), rainfall and snowfall distribution (Bintanja and Andry, 2017) and vegetation dynamics (Forkel et al., 2016). Minor temperature increase in areas with seasonal snow cover can cause changes to the hydrological cycle (Mioduszewski et al., 2014), changes in mass and energy cycles at different scales, phenology shift (Jeong et al., 2011; Shen et al., 2014) and a prolonged growing season (Blume–Werry et al., 2016; Delbart et al., 2006; Pau et al., 2011). In the northern hemisphere, snowmelt infiltration controls surface and subsurface hydrological processes (Ireson et al., 2013), refills soil water storage, provides water for root water uptake (Nehemy et al., 2022b; Sutinen et al., 2009b), and has a major role in groundwater recharge (Hyman–Rabeler and Loheide, 2023). The timing of snowmelt infiltration also limits the length of the growing season (Vaganov et al., 1999), while the total amount of plant available water in soil storage can be limited by the interplay of meltwater amount and soil characteristics (Muhic et al., 2023; Smith et al., 2011).

Due to challenging working conditions, understudied cryogenic fractionation processes (Beria et al., 2018; Evans et al., 2016), the constantly reducing number of research sites (Laudon et al., 2017), and an overall lack of field observations (Ala–Aho et al., 2021a), studies that implement stable isotopes of water have been less frequent at high latitudes (Tetzlaff et al., 2015). Still, the strong contrast between isotopic signals of enriched summer and depleted winter precipitation in sub-arctic areas (Dansgaard, 1964; Rozanski et al., 2013) and the relative isotopic depletion of accumulated snowpack and snowmelt compared to the rest of the hydrological system can serve as a potent tool for ecohydrological research. The substantial contrasts between snowmelt, typically observed values in the soil-vegetation interface during the summer season, and artificially enriched water are exploited in this study to create a double irrigation experiment. We used water labeled with

https://doi.org/10.5194/egusphere-2023-884
Preprint. Discussion started: 19 June 2023
© Author(s) 2023. CC BY 4.0 License.

deuterium to create a large, isotopically enriched infiltration event, and track water fluxes of different mobility at the soil-vegetation interface in order to identify the mechanisms of soil water replenishment. We further monitored the evolution of this isotopically enriched soil water pool during the winter, spring snowmelt, and one summer season to ascertain the role of snowmelt in restoration of soil water storage. The main objective of the study was to identify how sub-arctic forest till soils respond to infiltration events of high magnitude and explain the unique role of snowmelt in cold climate settings. The main research questions were:

1. What mechanisms control infiltration patterns in sub-arctic forest till soils?
2. How is spring snowmelt different from an artificial irrigation event of a similar size in soil water dynamics?
3. How do sub-arctic trees respond to extensive infiltration events?

## 2 Methods and data

### 2.1 Study site

The study site is in Pallas, a 4.42 $km^2$ headwater catchment within the sub-arctic climatic region of northern Finland (Fig. 1b, Marttila et al., 2021). The catchment elevation ranges from 270 to 360 m a.s.l. In 2003–2019 period, the mean annual air temperature at Pallas was 0.4 °C, and the long term monthly mean temperature was -11.3 °C in January and +13.9 °C in July. Mean annual precipitation in the 2008–2019 period was 647 mm/year, of which ~42 % fell as snow. Snowmelt onset varies from year to year, but usually occurs in May and early June.

https://doi.org/10.5194/egusphere-2023-884
Preprint. Discussion started: 19 June 2023
© Author(s) 2023. CC BY 4.0 License.

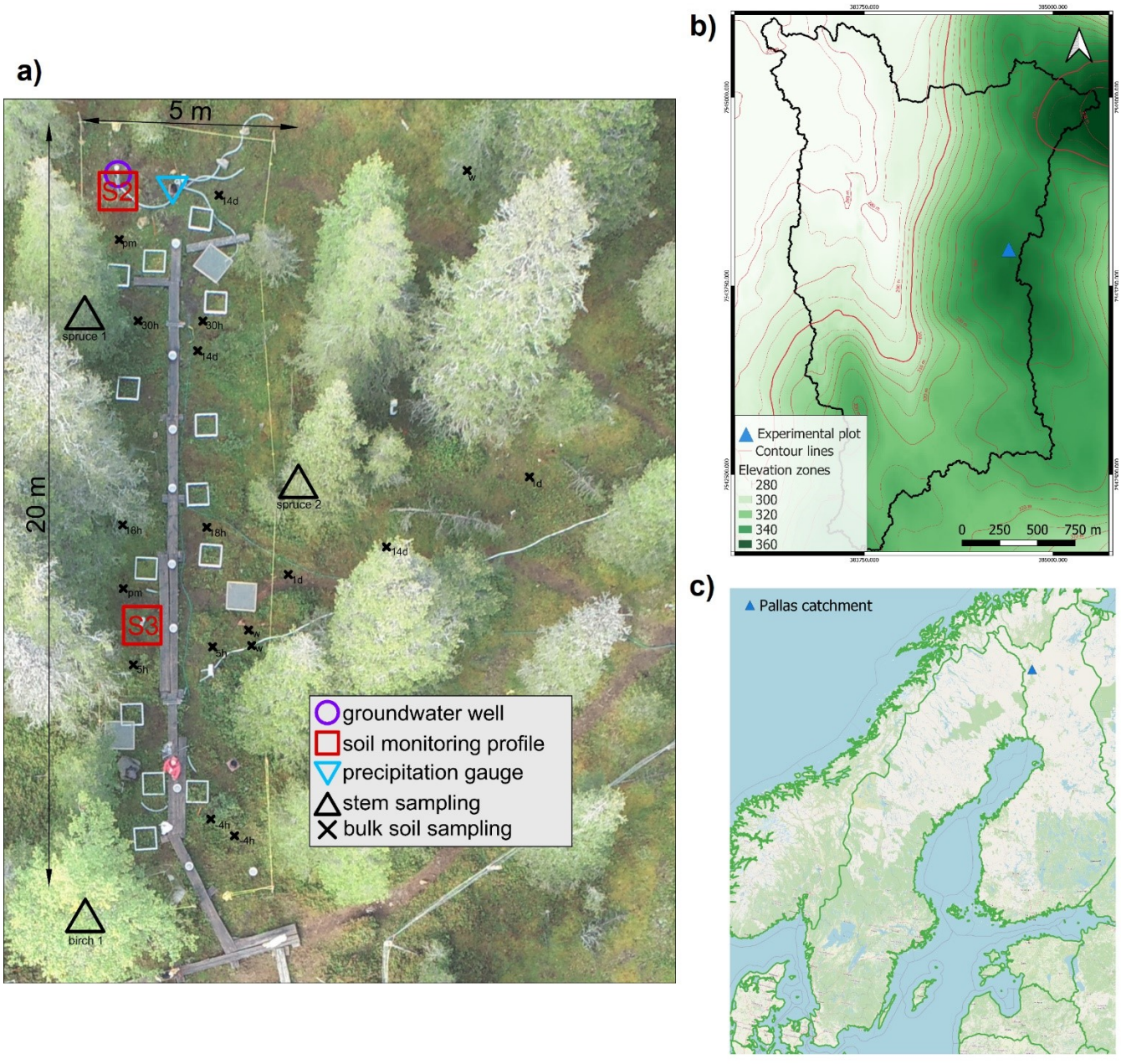


**Figure 1. Study site overview (a) Sketch of experimental plot with soil flux monitoring installations. Subscripts next to the bulk soil sampling locations denote sampling time ("w" and "pm" denote winter 2020 and post-melt 2020 periods, respectively, while "h" and "d" denote time since the start of experiment in hours or days). Aerial image by Bastian Steinhoff–Knopp (Leibniz University Hannover, September 2018); (b) Topographic map of the study catchment; and (c) Location of the study catchment within Northern Europe (blue symbol, 68° N, 24.2° E)**

https://doi.org/10.5194/egusphere-2023-884
Preprint. Discussion started: 19 June 2023
© Author(s) 2023. CC BY 4.0 License.

The 5x20 m experimental plot (EP) (Fig. 1a, Fig. 1b) is located at Kenttärova, a forested hilltop at the highest point in the catchment (67°59.237' N, 24°14.579' E, 347 m a.s.l.). The soil at the EP is shallow (less than 2 m depth) and consists of unconsolidated, podzolized tills and sandy tills (Fig. S1). The underlying granodiorite bedrock is heavily fractured and can be porous up to 10s of meters (Johansson et al., 2011).

Soil saturated hydraulic conductivities, estimated using the falling head permeameter method, range from $1.40 \cdot 10^{-6}$ m/s to $1.25 \cdot 10^{-5}$ m/s (n = 4) at a 5–10 cm depth, and from $9.78 \cdot 10^{-7}$ m/s to $8.92 \cdot 10^{-6}$ m/s (n = 3) at a 30–35 cm depth. Deeper soil samples for hydraulic conductivity tests could not be obtained due to the soil compaction and stoniness. Soil dry bulk density and porosity were determined after the pF curve test using a 5 bar pressure plate extractor CAT #1600 (SOILMOISTURE equipment co., Santa Barbara, CA, USA). Mean dry bulk density increases from 0.97 g/cm$^3$ at 5–10 cm to 1.86 g/cm$^3$ at 60–65 cm depth, and mean porosity from 0.53 (n = 4) to 0.26 (n = 3). Mean soil organic matter content, calculated after burning the soil samples at 550 °C in the muffle furnace (Nabertherm Naber N50 model), gradually reduces from 10 % at 5–10 cm, to 2.65 % at 30–35 and were less than 1 % below 60 cm depth. Based on soil temperature and frost depth monitoring and previous research by Sutinen et al. (2009a), we can see that soils at Pallas can experience seasonal freezing at a surficial frost depth. However, soil temperatures within the EP stayed above 0.25 °C during the study period (Fig. S2). Mean annual snowpack depth at this location, measured since 2008, was 105 cm (Lohila et al., 2015), but the 2019–2020 winter was unusually snowy and the maximum observed snowpack depth was 130 cm (Noor et al., 2023). The tree stand consists of Norway spruce (Picea abies), with a live canopy that covers almost the entire length of the tree stem, and pubescent birch (Betula pubescens) (Aurela et al., 2015).

Two soil profiles (S2 and S3 in Fig. 1a) in the EP were instrumented using time-domain reflectometry soil moisture and temperature sensors (Soil Scout, Soil Scout Oy, Finland) and PTFE/quartz suction lysimeters (PRENART SUPER QUARTZ standard, PRENART Equipment ApS, Denmark) at a 5, 30 and 60 cm depth. A self-made stainless-steel pan lysimeter of 20x30 cm size was installed at a 35 cm depth and connected via a PTFE tube to the 1 L sample-collecting bottle that was placed at a 1 m depth. Additionally, a 1.3 m deep groundwater well, screened at the bottom 40 cm, and a tipping bucket precipitation gauge with GP-HR general purpose logger (TruTrack, UK) were installed next to the S2 profile. Soil property characterization and all field installations, other than the precipitation gauge setup, were completed in May and June 2018, thus providing a full year for the instruments to equilibrate with the soil and minimize any structural disturbance before the irrigation experiment commenced.

### 2.2 Irrigation experiment

We conducted an irrigation experiment at the EP in late August 2019 (Aug 27 16:00 h – Aug 29 22:00 h). Once every 1–2 hours, a 1000 L water tank was filled with tap water spiked with 35 mL of 99.999 % deuterium oxide ($D_2O$) and was transported to the site and distributed around the EP using two sprinklers. The initial plan was to apply ~240 mm of water labeled with deuterium, an amount that roughly corresponds to a typical snowmelt event at Kenttärova, based on a 1 m deep snowpack with a snow water equivalent of ~0.24. Water ponding on the soil surface was first observed after 12 hours, and

https://doi.org/10.5194/egusphere-2023-884
Preprint. Discussion started: 19 June 2023
© Author(s) 2023. CC BY 4.0 License.

the irrigation was stopped once the surface ponding started extending downslope of the EP. The total duration of the irrigation was 30 hours and 163.6 mm of deuterated water, as recorded by the tipping bucket precipitation gauge, was applied to the EP. The mean (± standard deviation) weighted $\delta^2$H value of the irrigation water was 79.38 (±5.3) ‰ (Fig. 2a). The temporal variability of the irrigation intensity ranged between 2 and almost 11 mm/h, and led to fully saturated conditions in the EP soil. During irrigation, a 600 kPa vacuum was continuously applied to the suction lysimeters, as samples were collected hourly. Groundwater and pan lysimeter samples were sampled concurrently with suction lysimeters. Samples of the ponded surface water were sampled opportunistically.

Soil cores from the EP were collected 4 times during the experiment, using a percussion drill (Cobra 148, Atlas Copco) with a window sampling tube extension (RKS with a reinforced cutting edge with a core cutter Ø80 mm x 1 m, GEOLAB Paweł Szkurłat). Two replicate cores were collected each time and all cores were sampled at 5 cm increments down to a 50 cm soil depth and at 10 cm increments from a 50–100 cm depth. Stem samples of three trees located in the EP (indicated as birch 1, and spruce 1 and 2 in Fig. 1a) at a ~2 m height were collected each day of the experiment, 5 more times over the next 20 days, and once more after the 2020 snowmelt. More details about the bulk soil and stem sample handling in the field are provided in Muhic et al. (2023).

### 2.3 Long-term data collection

Soil temperature and volumetric soil moisture were measured every ~20 minutes and the groundwater level was measured every 10 minutes using a water level logger (Solinst levelogger, Solinst Canada Ltd., ON, Canada). We sampled the suction lysimeters for stable water isotopes every two weeks during the summer season in 2019 and 2020, and every two days, if there was any water available, during the snowmelt 2020 by applying 600 kPa of suction for a period of ~4 hours with a portable vacuum pump/compressor system (PRENART Equipment ApS, Denmark). Pan lysimeter water samples for isotope analysis were collected simultaneously with a hand operated vacuum pump, while groundwater was occasionally sampled with a bailer. Soil coring campaigns monitoring the seasonal changes in the EP were conducted 2 weeks after the experiment, at the peak snowpack in April 2020 and after 2020 snowmelt in mid June. Soil cores downslope of the EP were collected 1 day after the experiment, and again 2 weeks later and under deep snowpack in April 2020.

### 2.4 Supplementary data

Supplementary isotopic data used in the study includes stable water isotope ratios ($^2$H) of rainfall, snowmelt and bulk soil. Event-based rainfall samples were collected manually and using an automatic ISCO sampler (Model 6712, Teledyne ISCO, NE) located 2 km nortwest from the EP. Snowmelt samples from a snowmelt lysimeter situated within 100 m of the EP were collected daily throughout the melting periods in 2019 and 2020 (Noor et al., 2023). Bulk soil water samples were collected from a nearby (<100 m) forested plot (location SF1 in Muhic et al., 2023) on 3 occasions after the experiment and were used to assess the difference between irrigated and natural bulk soil water isotope composition. Additional hydrometric data is comprised of precipitation amount, air humidity, surface air temperature and net radiation data at 10-minute intervals,

https://doi.org/10.5194/egusphere-2023-884
Preprint. Discussion started: 19 June 2023
© Author(s) 2023. CC BY 4.0 License.

obtained from an eddy flux tower located immediately next to the EP, and snowmelt flux data from the aforementioned snowmelt lysimeter. Air vapor pressure deficit was calculated using the hourly air temperature and humidity using the formula from Foken (2008).

### 2.5 Isotope analysis

We used the direct equilibration method (DVE), as described in Wassenaar et al. (2008), to measure the isotopic composition of bulk soil water using a cavity ring-down spectroscopy (CRDS) analyzer (Picarro L2140-i model, Picarro Inc., Santa Clara, CA, USA) located at the University of Oulu. Mean standard deviations for $\delta^{18}O$ and $\delta^{2}H$ values were 0.114 ‰ and 0.284 ‰, respectively. We refer to Muhic et al. (2023) for a detailed description of the analysis procedure. Isotopic signature of liquid water samples from the groundwater well and suction and pan lysimeters were analyzed using the same Picarro analyzer, combined with an autosampler and a vaporizer unit.

Tree stem water was extracted by cryogenic vacuum distillation (CVD) method at the University of Utah Biology Department (Salt Lake City, Utah) following the protocol described by West et al. (2006) and Bowling et al. (2017). The extraction was facilitated using a hot bath filled with water at 100 °C, and extraction times ranged between 60 and 90 minutes. The extracted stem water was subsequently treated with activated charcoal for 48 hours. The isotopic composition ($\delta^{18}O$ and $\delta^{2}H$) of the stem water was measured on a Picarro L2130-i CRDS analyzer, and ChemCorrect software was used to examine possible sample contamination.

The isotopic composition of all samples was determined relative to the Vienna Standard Mean Ocean Water international standard, and shown in δ notation, according to Craig (1961) and Gonfiantini (1978).

## 3 Results

### 3.1 Soil water fluxes during the irrigation experiment

The $\delta^{2}H$ values of water fluxes at the EP, observed before the irrigation (-4 h), during the irrigation (0–30 h), and in the following 3 days after the irrigation was finished (30–89 h) are shown in Fig. 2. We refer to the 0–30 h period as the irrigation period and to the 0–89 h period as the experiment.

https://doi.org/10.5194/egusphere-2023-884
Preprint. Discussion started: 19 June 2023
© Author(s) 2023. CC BY 4.0 License.

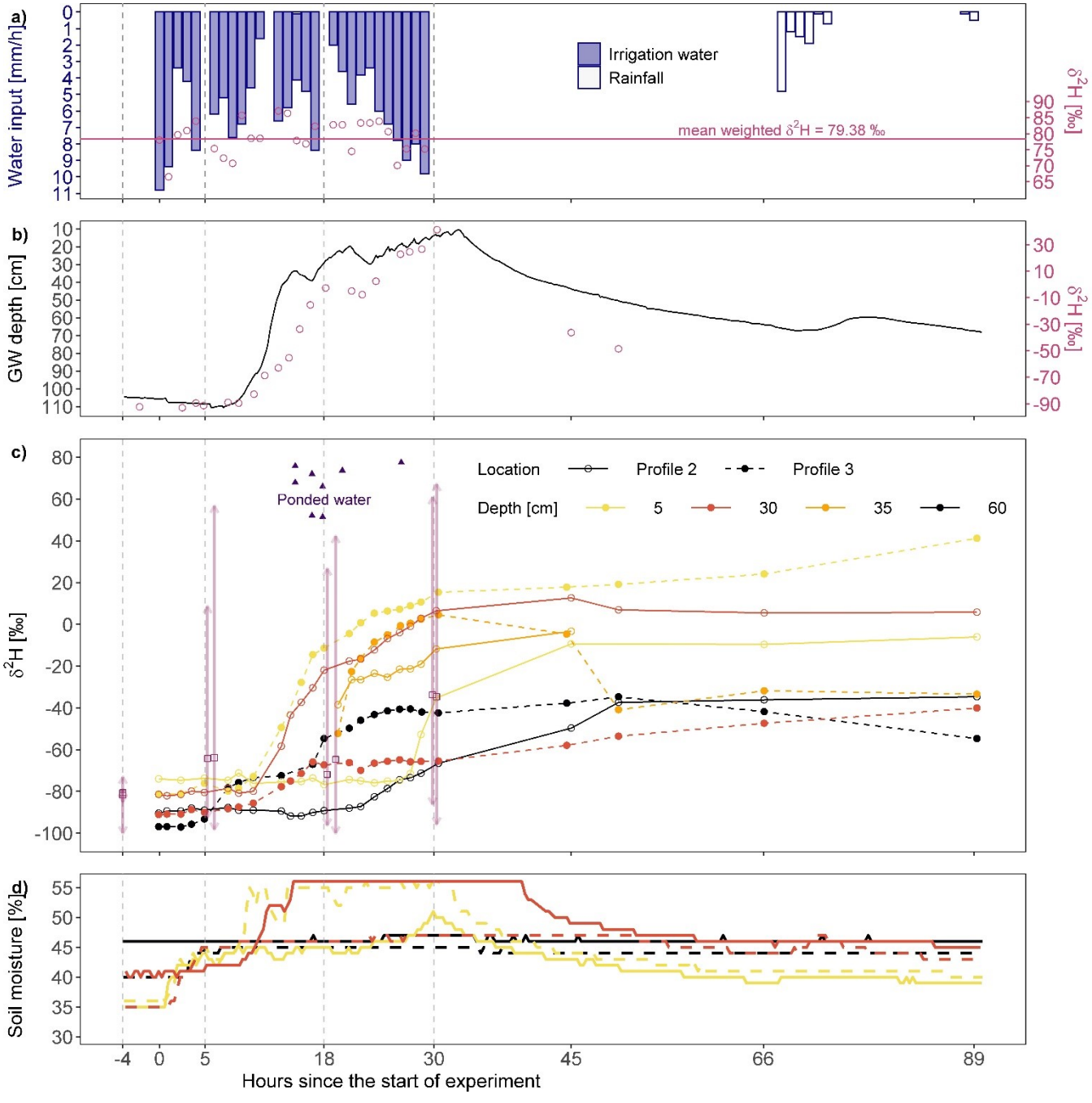


**Figure 2. Soil water dynamics during the irrigation experiment. (a) Hourly water input intensity (bars). The dots show $\delta^2$H values of irrigation water and the vertical dashed grey lines indicate the timing of bulk soil sampling; (b) Groundwater table dynamics, dots representing $\delta^2$H values of groundwater; (c) Soil water $\delta^2$H signal. Suction lysimeters are at 5, 30 and 60 cm depth. The orange lines and dots (35 cm depth) show pan lysimeter data, the purple arrows denote bulk soil $\delta^2$H variability, while the purple squares show the mean values; d) Volumetric soil moisture.**

https://doi.org/10.5194/egusphere-2023-884
Preprint. Discussion started: 19 June 2023
© Author(s) 2023. CC BY 4.0 License.

The groundwater level (Fig. 2b) was 110 cm below the surface at the start of the experiment and started to rise rapidly after 8 hours. The rate of groundwater level rise went down after reaching a ~35 cm depth, but the level generally continued to rise until 4 hours after the end of irrigation, reaching up to 11 cm below ground surface. The groundwater $\delta^2H$ signal was strongly correlated with both the groundwater level (Mann–Kendall $t = -0.83$, $p < 0.01$) and the total amount of applied irrigation water ($t = 0.92$, $p < 0.01$). The isotope ratio of the water sampled from the pan lysimeters (grey dots and lines in Fig. 2c) in both soil profiles responded to irrigation only after the groundwater level went up to their installation depth (35 cm). Ponded water samples were more enriched than the groundwater or soil water, and closely resembled the labeled water signal.

At the onset of irrigation, the isotope ration of water sampled from the suction lysimeter showed a gradual change from an isotopically more enriched signal in the upper soil (yellow lines in Fig. 2c) to a depleted signal at the deepest measurement points (black lines in Fig. 2c). The suction lysimeter samples were in a similar isotopic range as the bulk soil water samples (brown vertical lines in Fig. 2c). During the irrigation, the isotopic signals in the two monitored profiles differed greatly, especially at 5 and 30 cm depths. 10 hours after the start of the experiment, $\delta^2H$ signals from the suction lysimeters in profile 3 at 5 cm and profile 2 at 30 cm started becoming more enriched relatively quickly compared to the other locations. On the other hand, suction lysimeters in profile 2 at 5 cm and profile 3 at 30 cm showed no significant isotopic change, despite the full saturation of the EP evident from surface water ponding and high groundwater level. The fastest isotopic response in the EP was observed at a 60 cm depth (dashed black line in Fig. 2c) after only 5 hours. Soil moisture and isotopic dynamics were well synchronized at all sampling locations during the experiment, as the increase in soil moisture was followed by the enrichment in deuterium of the water sampled using the suction lysimeter. These paired dynamics were decoupled after irrigation stopped. Although more than 160 mm of water was applied, soil moisture in some relatively shallow layers (profile 2 at 5 cm and profile 3 at 30 cm depth) did not reach saturation values.

The EP was used in another irrigation study in 2019, with the aim of increasing the overall soil water content at the plot (Korkiakoski et al., 2022). Due to the frequent irrigation using tap water with a constant isotopic signal, bulk soil water $\delta^2H$ depth profile variability (Fig. 3) was relatively low at the start of the experiment. Topsoil isotopic values were enriched quickly, as a substantial change in the top 20 cm of soil was observed in the first collected samples 5 hours after the start of irrigation. Isotopic profiles then barely changed between 5 and 18 hours, despite having ~60 mm more irrigation water applied. In fact, the signal at a 10–20 cm depth became more depleted. Still, at the end of irrigation, at the 30–hour mark, the bulk soil water $\delta^2H$ signal in the top 15 cm was strongly enriched, and traces of deuterated water could be observed down to a 45 cm depth. The bulk soil water in the upper layers was constantly more enriched than the soil lysimeter water, even compared to the lysimeter samples taken up to 2 hours after soil coring. In fact, the bulk soil water $\delta^2H$ signal collected at the 5-hour mark was more enriched than any soil lysimeter $\delta^2H$ signal detected during the whole observation period. Opposite dynamics were present in deeper (below 30 cm) soil layers, where lysimeter waters showed a more enriched signal.

https://doi.org/10.5194/egusphere-2023-884
Preprint. Discussion started: 19 June 2023
© Author(s) 2023. CC BY 4.0 License.

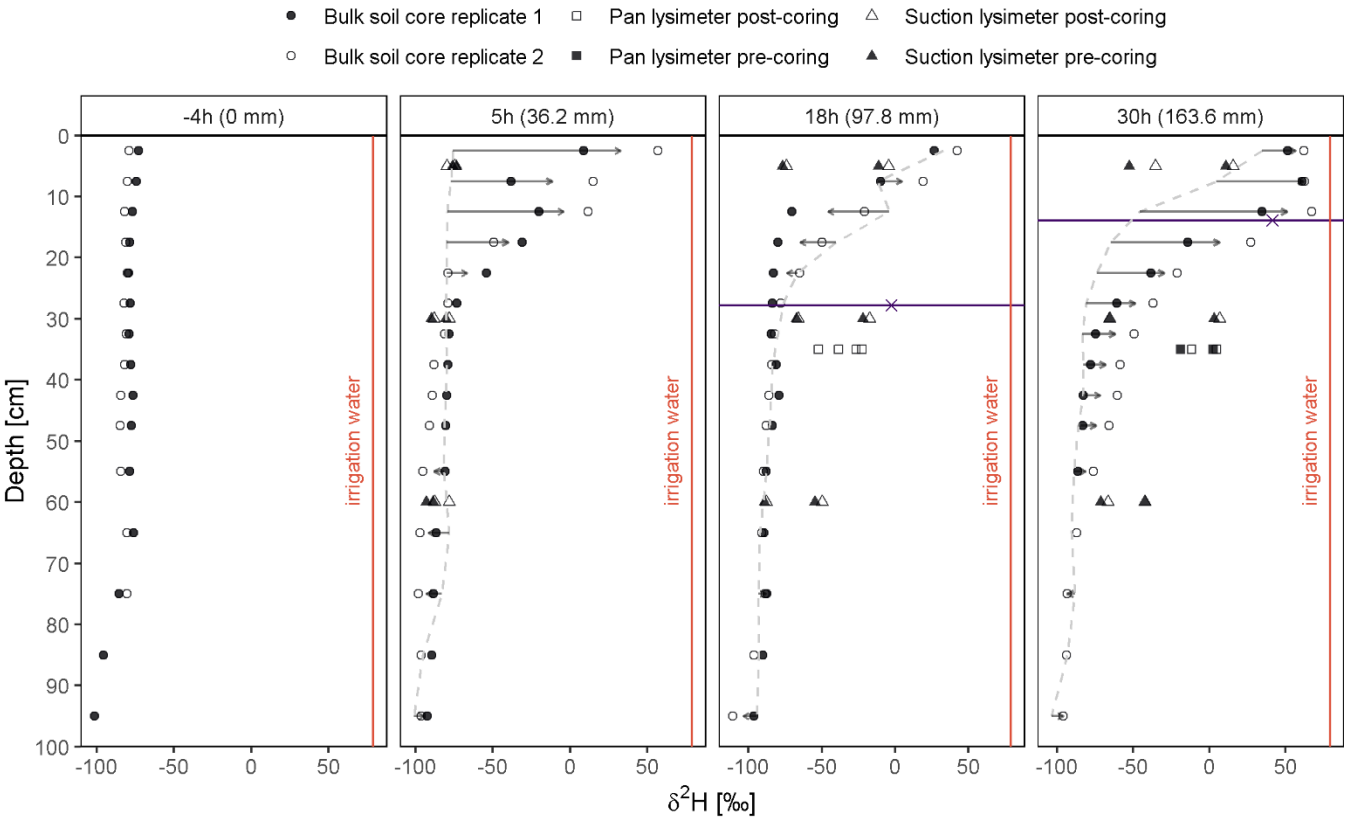


**Figure 3. Bulk soil water $\delta^2$H dynamics during the experiment (dots). Triangles denote soil lysimeter $\delta^2$H values collected within 2 hours before (pre-coring) and after (post-coring) bulk soil sample collection. The difference and direction of isotopic changes between the mean values of current bulk soil isotopic profiles and previously sampled (grey dashed line) isotopic profiles are indicated by arrows. The horizontal line shows groundwater level, and groundwater isotopic composition is marked on the line.**

### 3.2 Changes in soil water fluxes and isotope values after the experiment

The 2020 winter season was characterized by a distinctively deep snowpack (Noor et al., 2023) and a subsequent snowmelt event of above-average size (~350 mm) (Fig. 4a). During the snowmelt, the groundwater level in the EP stayed close (up to 10 cm) to the surface for ~2 weeks. After this, it displayed a quick drawdown followed by another short-lasting peak (Fig. 4b). Soil moisture levels remained relatively high throughout the observation period, and there was a notable soil moisture increase at all depths and in all profiles during the snowmelt event. The first soil lysimeter water samples, collected at the onset of snowmelt, were still strongly enriched compared to the values that are naturally observed in Pallas soils (Muhic et al., 2023), due to a portion of irrigation water remaining in the soil over the winter (Fig. 4d). The most enriched values were observed in deeper soil, while topsoil isotopic composition was strongly depleted. The enriched water was gradually and fully removed during the snowmelt (zoomed in part in Fig. 4d), as the isotopic variability of soil waters sampled using suction lysimeters was continuously reduced and converged towards snowmelt values. Consequently, soil water isotopic dynamics for the rest of the summer resembled the previous summer's dynamics (Fig. S3), as the $\delta^2$H values were steadily

https://doi.org/10.5194/egusphere-2023-884
Preprint. Discussion started: 19 June 2023
© Author(s) 2023. CC BY 4.0 License.

enriched through the summer, with deeper lysimeters showing more depleted signal than the lysimeters in the upper soil.

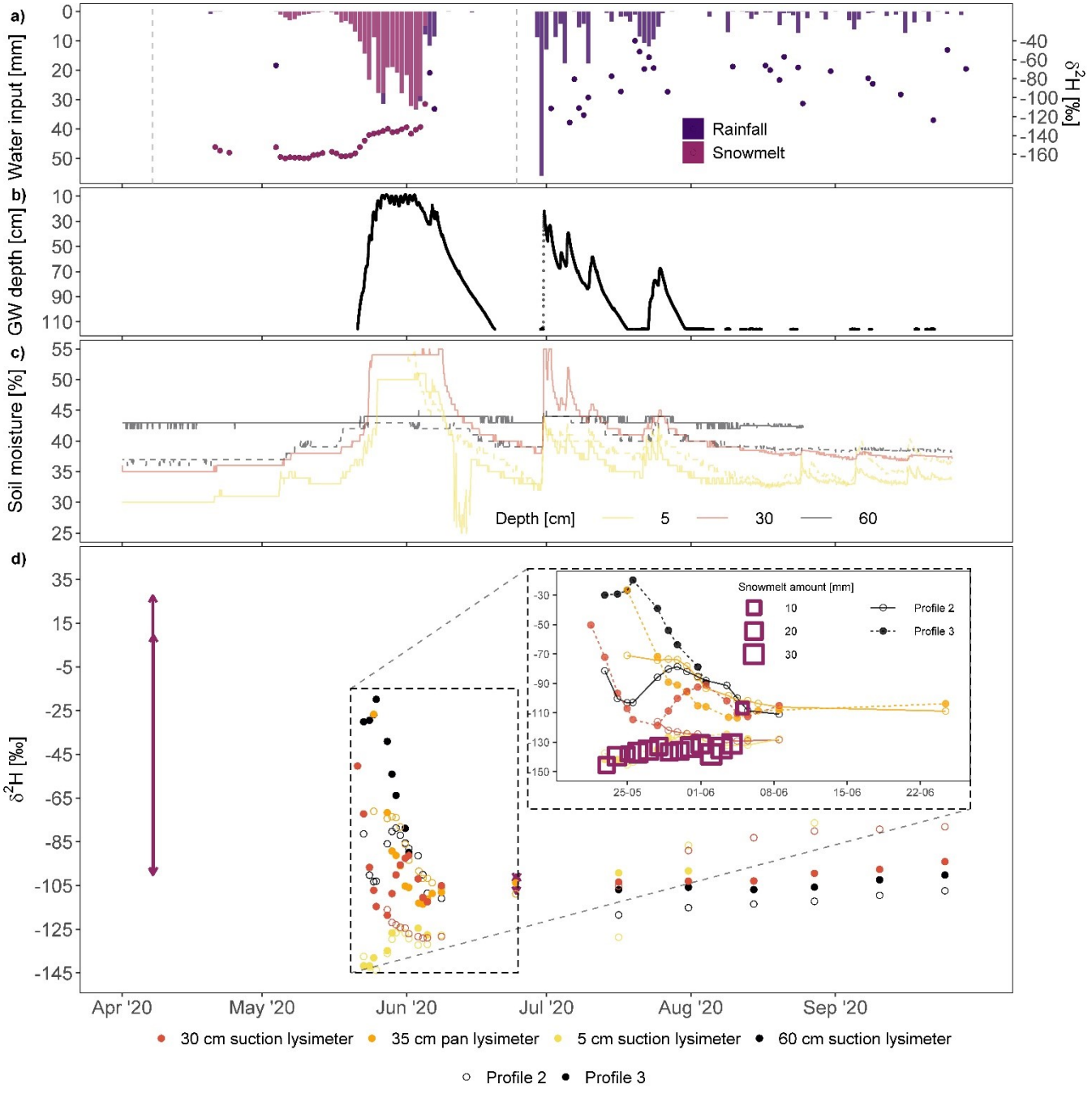


**Figure 4. Water fluxes at the irrigation plot during the whole observation period. (a) Infiltration event magnitude (bars) and $\delta^2H$ signal (dots). The dashed grey vertical lines show soil coring campaign timings; (b) Groundwater table dynamics; (c) Volumetric soil moisture; (d) Soil water $\delta^2H$ signal. The range of bulk soil $\delta^2H$ values is indicated using purple arrows. The insert graph displays soil lysimeter water and snowmelt water isotopic dynamics during the snowmelt period.**

https://doi.org/10.5194/egusphere-2023-884
Preprint. Discussion started: 19 June 2023
© Author(s) 2023. CC BY 4.0 License.

The effect of irrigation on the bulk soil water isotopic signal was assessed by comparing the observed $\delta^2H$ values in the EP, a nearby reference plot not affected by irrigation, and an area downslope of the EP (Fig. 5). In the EP, autumn rainfalls fully shifted the strongly enriched signal in the upper (<10 cm) soil layers towards the values observed in the reference plot (yellow lines in Fig. 5). The deuterium peak moved down to a 32.5 cm depth and enriched values were also observed at a 95 cm depth (second panel in Fig. 5a). The depth distributions of $\delta^2H$ in 2 soil cores from the EP were similar, but $\delta^2H$ values were more enriched in the EP replicate 1 (Fig. 5a). The $\delta^2H$ depth dynamics in soil cores from the winter period showed more resemblance to the cores obtained in the non-irrigated plot, with comparable values in the upper 40 cm, while the peak dropped to 90–100 cm. After the snowmelt, the $\delta^2H$ signals in EP were as depleted as the signal in the reference plot, with near-identical signals detected at all 4 cores.

The lateral fluxes which resulted from the irrigation experiment are displayed in Fig. 5b. Two soil cores were excavated 1 day after irrigation ended (see Fig. 1), one immediately next to the EP (light grey dots, first panel in Fig. 5b), in the zone affected by surface water ponding, and the other 10 m downslope (dark grey dots, first panel in Fig. 5b). The effect of surface water ponding can be clearly identified in the upper 10 cm of soil, but depth dynamics of deuterium below a 10 cm depth were remarkably similar, and a small peak (~ -17 ‰ $\delta^2H$) was present at a 20 cm depth. As in EP, autumn rainfall shifted the $\delta^2H$ signal in upper soil towards the natural range (14 days after irrigation), but the deuterium breakthrough curve peak moved downwards at a faster rate than in the EP. In winter, soils in the EP and downslope of the EP showed similar $\delta^2H$ depth dynamics, but the signal in deeper soil layers (below 60 cm) was more enriched in the EP.

https://doi.org/10.5194/egusphere-2023-884
Preprint. Discussion started: 19 June 2023
© Author(s) 2023. CC BY 4.0 License.

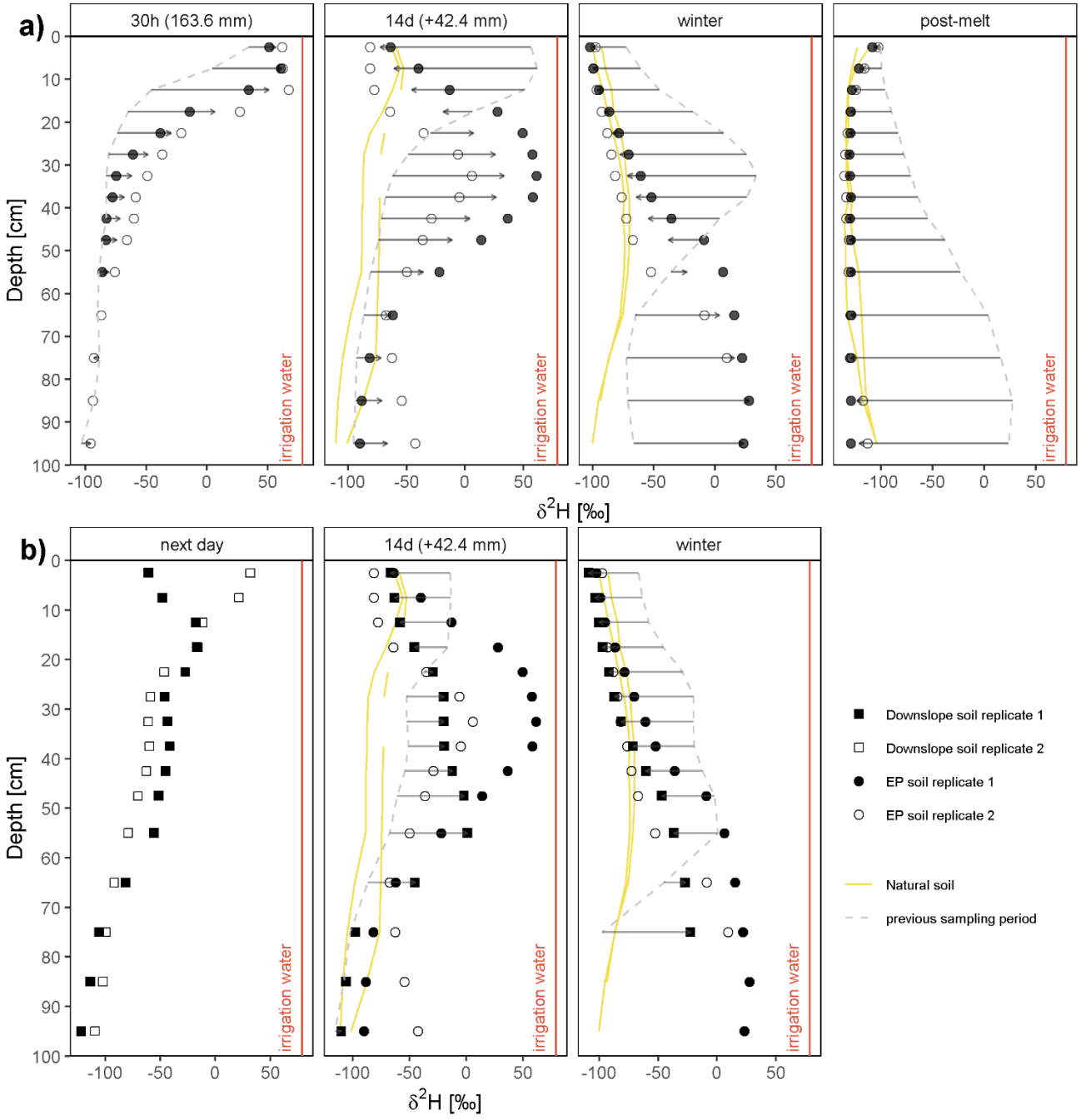


**Figure 5. Bulk soil water $\delta^2$H dynamics after the experiment in the (a) Irrigation plot, and (b) in soil immediately downslope of the EP. Yellow lines show bulk soil water dynamics in a nearby reference plot, collected at the same time. The isotopic change between the mean values of current isotopic profiles (dots) and the previously sampled (dashed line) mean isotopic profile in the EP are indicated using arrows. Bulk soil $\delta^2$H values collected from the EP in the same period are displayed for comparison.**

https://doi.org/10.5194/egusphere-2023-884
Preprint. Discussion started: 19 June 2023
© Author(s) 2023. CC BY 4.0 License.

### 3.3 Bulk stem water $\delta^2$H dynamics

The trees for stem water sampling were selected in 2018, but the irrigated zone was moved slightly in 2019, leaving the birch tree 30–40 cm outside of the irrigation zone (Fig. 1a). Nevertheless, it can be assumed that the lateral spread of the birch tree's roots is large enough to reach the irrigation zone. $\delta^2$H values of samples obtained before the irrigation event were clustered around -75 ‰ (-74.61, -72.70 and -78.00 ‰), but the stem water dynamics of birch and spruce trees were different during the experiment. The birch tree did not respond strongly to the irrigation event, as the stem water isotopic signal remained mostly stable throughout 2019, while the spruce stem water dynamics were characterized by two peaks; a smaller one ($\Delta\delta^2$H of +4 ‰ and +12 ‰) at the end of irrigation (Fig. 6b, day 1) and a larger one after 15 days ($\Delta\delta^2$H up to +80 ‰ compared to the pre-irrigation signal). In the summer of 2020 (day 302 after the start of the experiment), all samples displayed a strongly depleted $\delta^2$H signal again (~-112 ‰), comparable to the $\delta^2$H signal observed in both bulk and lysimeter soil water.

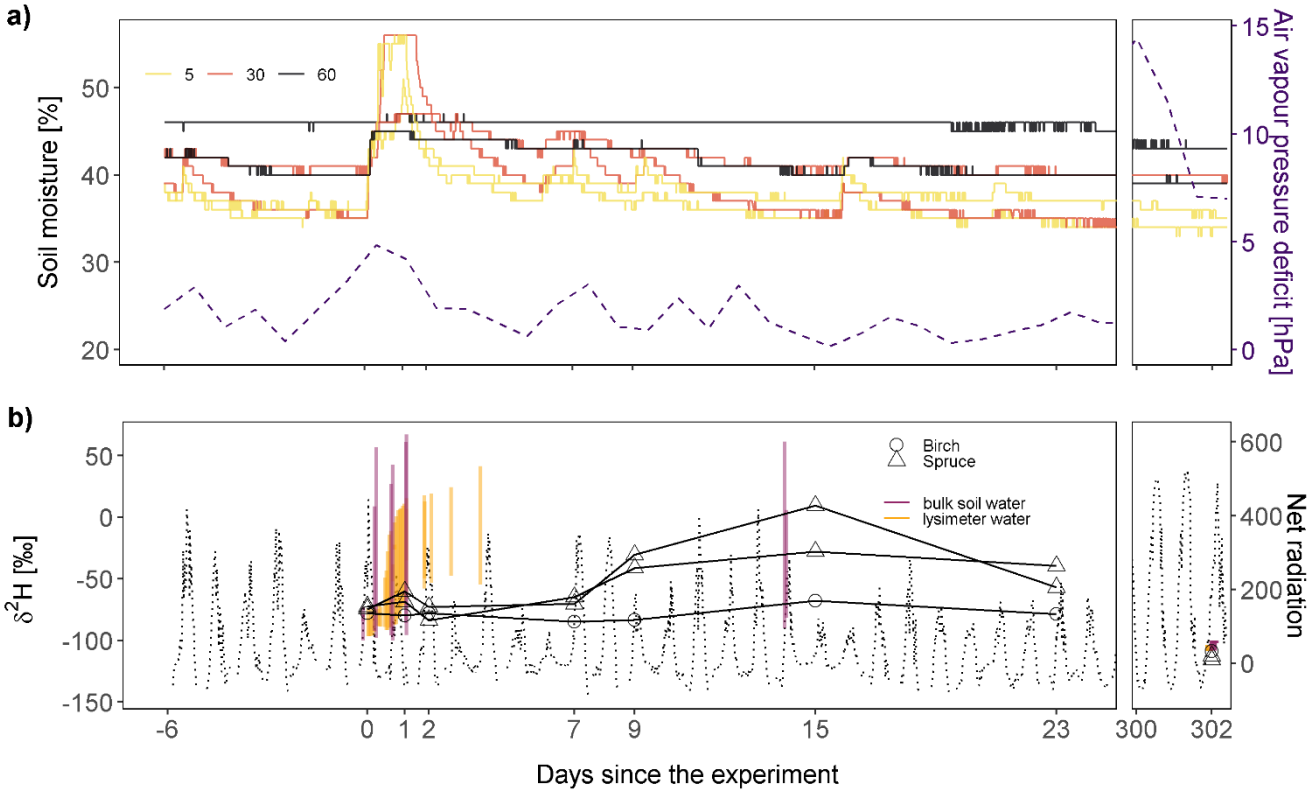


**Figure 6. Water fluxes at the soil-vegetation interface. (a) Volumetric soil moisture (solid lines) and air vapor pressure deficit (dashed line) dynamics; (b) The bulk stem water isotopic signal (solid lines and triangles) and net radiation (dashed lines). The vertical orange lines show the $\delta^2$H variability of soil lysimeter water, while purple vertical lines show the $\delta^2$H variability of bulk soil water.**

https://doi.org/10.5194/egusphere-2023-884
Preprint. Discussion started: 19 June 2023
© Author(s) 2023. CC BY 4.0 License.

## 4 Discussion

We simulated an infiltration event similar to snowmelt on an experimental plot with shallow till soil, located on a forested hilltop in a sub-arctic zone, by applying 160 mm of deuterated water over a 30-hour period. The resulting soil water fluxes displayed high spatiotemporal variability, identifiable in both hydrometric and isotopic data. We further observed fast groundwater table rise, bypass flow, and surface water ponding during the irrigation. An isotopically enriched signal was preserved in the soil storage throughout the winter period, and then got fully flushed out by the spring snowmelt, leading to strong isotopic homogenization of the soil. Observed soil water fluxes at the soil-vegetation interface uncovered infiltration mechanisms in shallow arctic till soils and highlighted the unique role of snowmelt in soil water replenishment. We detected three infiltration stages (Fig. 7):

1) First stage – the initiation of macropore flow: Surface microtopography induces surface ponding and focused infiltration. Infiltrating waters first fill the soil matrix, but once the infiltration capacity of surficial soil matrix is exceeded, the water fluxes are conveyed downwards through the macropore network. Fluxes are largely vertical and macropore flow is unsaturated.

2) Second stage – development of lateral fluxes: As the transport capacity of certain parts of the macropore network is surpassed, the flow is reversed, and groundwater rises towards the surface through the macropore network. Increased surface ponding generates surface flow via a fill and spill mechanism, while groundwater exfiltration to upper, more conductive soil layers initiates subsurface lateral flows through a transmissivity feedback mechanism. Buildup of pressure in the saturated macropores leads to increased horizontal hydrologic connectivity in the macropore network. Isolated and air-filled macropores, as well as a substantial part of the soil matrix, are still largely unaffected.

3) Third stage – soil matrix refilling: The constant water supply combined with a prolonged period of high groundwater table leads to increased hydrologic connectivity of the macropore network at all depths. Water diffusion into textural pores and pore water exchange between macropores and the soil matrix are bolstered due to the increased contact surface and increased time for dispersive exchange, thus promoting soil water homogenization and soil matrix flow, and further increasing soil wetness and hydraulic conductivity. Shorter distances between water-filled macropores and near-saturation hydraulic conductivity allow matrix flow to reach all soil pores.

https://doi.org/10.5194/egusphere-2023-884
Preprint. Discussion started: 19 June 2023
© Author(s) 2023. CC BY 4.0 License.

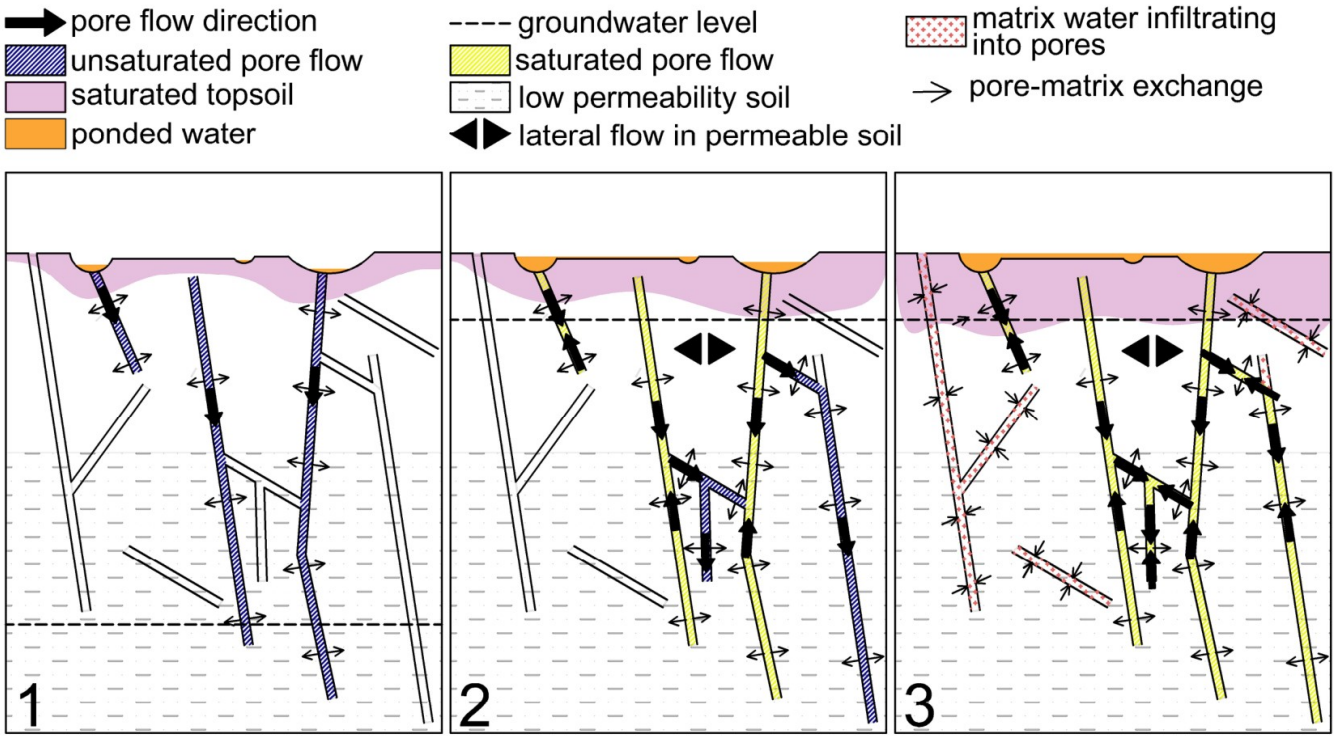


**Figure 7. Infiltration mechanisms in shallow sub-arctic till soil: (1) the initiation of macropore flow; (2) the development of lateral fluxes; and (3) refilling of soil storage.**

### 4.1 The initiation of macropore flow

Isotopic heterogeneity of soil waters is universally observed, and it would be advantageous to identify under what conditions isotopic homogeneity (Sprenger and Allen, 2020) and full soil matrix water displacement can be achieved. The amount of water applied to the soil during this experiment was relatively large, considering the shallow soil at this location, yet soil water storage continuously displayed a strong heterogeneity in soil moisture measurements (yellow and red lines in Fig. 2c). Our data shows that some soil patches at a 5 cm depth remained largely isolated from infiltrating waters for a long period (solid yellow and dashed red lines in Fig. 2d), despite isotopic changes in deeper soil layers already taking place and plot-wide surface water ponding. Such agreement between isotopic and hydrometric responses was also found by Laudon et al. (2004) in a study conducted in till soils overlaid by organic soil layers of different depths. The immediate increase of soil moisture and strongly enriched $\delta^2H$ signal in the upper layers of bulk soil samples collected after 5 hours, with no change in the isotopic composition of suction lysimeter water (Fig. 2c), suggest that, in agreement with soil physics principles, the slow

https://doi.org/10.5194/egusphere-2023-884
Preprint. Discussion started: 19 June 2023
© Author(s) 2023. CC BY 4.0 License.

domain (smaller pores in the soil matrix) is filled first (Hrachowitz et al., 2013; Hutson and Wagenet, 1995). Brooks et al. (2010) observed that infiltrating water first enters smaller pores, but the filling of smaller pores subsequently causes a decrease in soil matric potential, so the infiltrating water starts bypassing the soil matrix and moving through bigger pores and preferential flow pathways. Column studies under near-saturated conditions have further underlined the role of well-connected networks of smaller pores in preventing the initiation of macropore flow (Larsbo and Jarvis, 2005). In their dynamic partial mixing model, Hrachowitz et al. (2013) concluded that the relocation of flow to larger pores limits dispersive exchange between preferential flow pathways and the soil matrix by reducing the contact surface and contact times between these soil domains. Routing of water to preferential flow pathways can be additionally exacerbated under near-ponding conditions (Bogner et al., 2013; Kulli et al., 2003; Li et al., 2013), such as the ones observed in this study, due to limited soil infiltration capacity. The reduced interaction between macropores and the soil matrix may be one possible explanation for the offset between soil bulk and lysimeter waters sampled at the same time and depth (Fig. 3). Studies which have focused on the isotopic difference between bulk and lysimeter waters often had inconclusive results regarding the main drivers of this separation (Finkenbiner et al., 2022; Oshun et al., 2016; Sprenger et al., 2018a; Xiao et al., 2020), but agreed that the interaction between macropores and the soil matrix depends on soil characteristics (Scherrer et al., 2007). Isotopic offsets between bulk soil and soil lysimeter water have been estimated in previous studies using an empirical formula (Chen et al., 2016) and via an isotope mass balance approach (Sprenger et al., 2019), but strongly heterogeneous conditions in EP prevent the application of such formulas.

The infiltration capacity of soils is controlled by their soil texture, structure, antecedent moisture, microtopography and various site-specific processes (e.g., soil freezing), so different infiltration mechanisms and responses to excess infiltration are observed in different soils. Small scale variation of terrain and surface vegetation can cause focused infiltration and surface ponding, as observed during this experiment (Fig. S3). Small topographic depressions, varying in diameter from centimeters to meters, are often described as ground surface roughness (Hansen, 2000) and strongly impact surface connectivity, storage, overland flow (Darboux et al., 2002; Frei et al., 2010), and soil profile development (Manning et al., 2001). They are commonly observed in many sub-arctic landscapes (Hayashi et al., 2003), where they serve as temporary accumulation spots for meltwater and promote groundwater recharge and bypass flow through focused infiltration (Berthold et al., 2004; Hayashi et al., 2003). Although soil freezing blocks the pores in soil matrix, thus reducing the pore connectivity and hydraulic conductivity of the soil, macropores can remain air filled and enable preferential flow and rapid transport of the infiltrating water (Hayashi, 2013; Mohammed et al., 2018). Even in soils with high ice content, a well-developed network of large macropores can regulate the hydrologic response, hence the effect of soil freezing on infiltration rates is reduced in forested regions with deep snow cover, such as Pallas (Ala-Aho et al., 2021b). Focused infiltration in small (<1 m diameter) depressions was identified by French and Binley (2004). The highly enriched $\delta^2H$ signal of ponded water samples (Fig. 2c) collected in EP suggests that irrigation water was temporarily stored in these small depressions as infiltration excess, due to an inability to infiltrate deeper into the soil. In such periods of high soil saturation, preferential flow is usually intensified, as the water is increasingly transported through a small fraction of the total soil pore space (Jarvis, 2007), thus

https://doi.org/10.5194/egusphere-2023-884
Preprint. Discussion started: 19 June 2023
© Author(s) 2023. CC BY 4.0 License.

reducing its residence time in the system (Šimůnek et al., 2003). The occurrence of preferential flow is common in glacial till soils (Etana et al., 2013), especially at hilltop sites (Liu and Lin, 2015).

### 4.2 Development of lateral fluxes

We detected that fast groundwater level rise (Fig. 2b) strongly correlated with $\delta^2H$ increase of groundwater. Derby and Knighton (2001) described similar processes and detected the formation of groundwater mound and the swift transport of applied tracers beneath soil depressions. The strong correlation between groundwater level and isotopic signal illustrates how irrigation water mixes with the existing soil water storage, with the amount of mixing relative to the distance from the soil surface to the groundwater table. The observed rate of groundwater rise was significantly higher than the saturated hydraulic conductivity of the soil, indicating that groundwater moves via bypass flow through the macropore network. If the GW response resulted from Darcian matrix flow based on the saturated hydraulic conductivity of upper soil layers (mean value ~$5.70 \cdot 10^{-6}$ m/s), and under a 1m hydraulic gradient due to elevation, the rate of groundwater level increase would be ~0.5 m/day. This is an overestimation, because unsaturated conductivity is lower than saturated conductivity, and soils below 50 cm depth are significantly more compacted and less porous, so their conductivity can be several orders of magnitude lower. Furthermore, the deuterium peak in the depth profiles moved from 10 cm to 30 cm over the 14-day period after the experiment, and from 30 cm to 85 cm during the following ~6 months (Fig. 5a, panels 1–3). Despite such slow water transport through the soil matrix, we observed that the groundwater level increased by 77 cm during an 8-hour period, between hour 6 and hour 14 of the experiment. Although macropore flow is typically unsaturated due to its high transport capacity (Cey and Rudolph, 2009; Jarvis, 2007), we can assume that upward water flow signals the saturation of vertical macropores, and consequently intensifies the lateral movement of water and strengthens horizontal hydrological connectivity in the macropore network. While macropore flow is unsaturated, soil water does not enter the interconnected pores that spread laterally from the main macropore (Fig. 7, left panel). As the saturation level increases, macropore flow becomes more similar to piston flow, and the buildup of pressure instigates the movement of water into the laterally spreading pores (Fig. 7, mid panel). Weiler and Naef (2003) observed macropore system saturation due to low interaction between the macropores and soil matrix of low permeability, and a subsequent development of subsurface flow once the water table reached the more permeable topsoil layers.

Once the groundwater table reached the upper soil layers, lateral soil water fluxes greatly increased, which is evident by the reduction in the rate of groundwater level rise and the amount of water extracted from pan lysimeter sample collection bottles (~0.5 L per hour). As pan lysimeters did not receive any water in periods when groundwater level was below their installation depth (35 cm, Fig. 2c), it seems that the flow volume of the freely draining water was not sufficient to reach the sampling bottle. Accordingly, the water samples collected from the pan lysimeters during the experiment likely originate from lateral flow, rather than from freely draining water. The development of lateral fluxes due to groundwater rise is commonly observed in northern sub-arctic catchments with glacial till soil (Laudon et al., 2004; Stumpp and Hendry, 2012). Also, the basic requirements for the transmissivity feedback mechanism (Kendall et al., 1999), saturated hydraulic

https://doi.org/10.5194/egusphere-2023-884
Preprint. Discussion started: 19 June 2023
© Author(s) 2023. CC BY 4.0 License.

conductivity that increases towards the surface and near-surface soil horizons, are fulfilled in the EP (Section 2.1 and Table S1). Furthermore, the rate of groundwater table rise decreased as the groundwater level reached more permeable soil, despite the irrigation being applied at the same rate, revealing continuous water loss through lateral fluxes in shallow (~0–35 cm depth) soil layers. Bulk soil samples collected 14 days after the experiment (Fig. 5b, panel 2) revealed that the deuterium peak reached a greater depth downslope of the EP than in the EP, which can result from lateral transport caused by groundwater mounding (Stumpp and Hendry, 2012). After irrigation, the groundwater isotope signal recovery (depletion) was rapid, as the enriched retreating groundwater again mixed with the pre-event water from the soil storage (Fig. 2b). Groundwater table rise promotes more intense mixing with the water stored in the unsaturated zone (Rouxel et al., 2011), but the short duration of a high water table and its subsequent fast drawdown did not isotopically homogenize the soil. Negligible isotopic change in the deeper (below 45 cm) soil layers (Fig. 3) shows that the water fluxes in these layers are still largely transported through the macropore network. Aboveground water fluxes developed during the experiment, like the previously described surface water ponds, slowly expanded and merged into an ephemeral surface water network (Fig. S4), following the fill-and-spill mechanism (Appels et al., 2011; Tromp–Van Meerveld and McDonnell, 2006), which can produce biogeochemical hotspots (Frei et al., 2012) on a plot scale and promote surface-subsurface water exchange (Frei et al., 2010).

### 4.3 Soil matrix refilling

The deuterated water signal was fully removed from the topsoil after rainfall events following irrigation (Fig. 5), consistent with the findings of Rothfuss et al. (2015). The enriched signal remained deeper in the bulk soil during the winter and slowly travelled downwards, as deeper bulk soil water samples revealed a delayed response to the irrigation event. Traces of enriched water were also observed in lysimeter water at the onset of snowmelt (Fig. 4d) but were gradually depleted during the snowmelt. Essentially, the aftermath of this uncharacteristically large snowmelt event was the homogenization of all water fluxes at the soil-vegetation interface (Fig. 4d, right panel in Fig. 5b) and a marked decrease in soil water ages, as described in Sprenger et al. (2018b). This contrasts with the findings of Laudon et al. (2004), who identified no isotopic effect of 200 mm of snowmelt in glacial till soil layers below a 90 cm depth, possibly due to deeper (10 to 15 m) soils. Compared to this study, Sprenger et al. (2017) found that the peak bulk soil isotopic variability was perceived after massive infiltration events, but none of the considered events were comparable in scale to the snowmelt in our study. The potential of snowmelt to strongly flush the entire subsurface system and reset the isotopic values of soil waters was recognized in a recent study by Michelon et al. (2023).

The primary reason for such a drastic effect of snowmelt on the soil water storage is an extended period (more than 2 weeks) of a high groundwater table, combined with a constant snowmelt-sourced water supply (Fig. 4a and Fig. 4b). This long-lasting soil saturation enhances the imbibition rate of water into the smaller pores through an increased wetted area and promotes equilibrium conditions within the soil continuum by increasing short-range connectivity (Schlüter et al., 2012) and reducing water pressure fluctuations. With continuous water supply, individual macropore saturated zones can merge and

https://doi.org/10.5194/egusphere-2023-884
Preprint. Discussion started: 19 June 2023
© Author(s) 2023. CC BY 4.0 License.

saturate large volumes of the soil (Newman et al., 2004). Numerous studies have revealed that large air bubbles may remain trapped in the macropores (Sněhota et al., 2010), even during the gradual saturation of the soil from below (Luo et al., 2008), and remain non-conductive for water flow (Jarvis, 2007). This means that major part of the soil storage can only be replenished via slow soil matrix flow. Prolonged periods of a high groundwater table can further enhance matrix flow by augmenting soil hydraulic conductivity (van Genuchten, 1980) and, consequently, the soil matrix flow rates (Fig. 7). Such prolonged soil saturation is less likely to occur on steep slopes, Mueller et al. (2014) found highly spatially variable soil isotopic signals during the snowmelt period. Long-lasting soil saturation could also be less frequent in high-latitude areas in the future, as climate model simulations predict a precipitation shift from snowfall to rainfall (Bintanja and Andry, 2017). As demonstrated by the irrigation experiment, even large summer rainstorms are not likely to produce a long saturation period, due to their higher intensity and shorter duration. The findings highlight the unique role of snowmelt in replenishing and rejuvenating soil water storage.

### 4.4 The influence of vegetation on soil water fluxes

Besides soil characteristics and infiltration rates, soil water infiltration patterns and storage are also affected by vegetation, through species-specific hydraulic redistribution and water uptake (Dubbert and Werner, 2019). Plant water fluxes are controlled by the moisture gradient between the atmosphere and soil, and saturated soil conditions, present in northern regions during the snowmelt, often induce plant rehydration (Nehemy et al., 2022b) through positive root pressure (Hölttä et al., 2018). Root water uptake is a passive process that follows the water potential gradient, so saturated soils can drive the water into the roots. In such circumstance, internal plant water storage can be a significant outlet for soil water fluxes. Although the timing of the experiment was in a period with low net radiation and vapor pressure deficit (Fig. 6), we discovered an isotopic response in bulk stem water from a spruce tree within 30 hours of the start of irrigation, most likely caused by the inflow of water from the fully saturated soil. Such response was not observed in the birch tree that was located slightly outside of the EP, presumably because of the majority of its roots being in a non-irrigated zone. Soil saturation during the experiment was of a local character, as soil moisture in areas immediately upslope of the EP did not change (Fig. S5). $\delta^2H$ increase during the experiment noted in the second spruce tree (+4 ‰) was rather low and did not necessarily originate from labelled water, as heterogenous isotopic signals within the tree (Goldsmith et al., 2019; Seeger and Weiler, 2023; Treydte et al., 2021) can produce an offset of a similar size. However, it is also possible that the labeled water signal was diluted after mixing with the pre-existing water in the xylem (Aguzzoni et al., 2022). As the bulk stem waters were extracted using a cryogenic vacuum distillation method and analyzed using a laser spectrometer, the isotopic values could have also been affected by extraction biases (Diao et al., 2022) and co-extracted organic compounds (Martín–Gómez et al., 2015; Millar et al., 2018), while the true signal of sap flow could have been additionally masked by exchange with other water compartments within the stem (Barbeta et al., 2022; Fabiani et al., 2022; Nehemy et al., 2022a). The combination of the strong isotopic signal of irrigation water and the analysis that relies on relative isotopic changes in a brief period should limit the effect of the described biases on the results.

https://doi.org/10.5194/egusphere-2023-884
Preprint. Discussion started: 19 June 2023
© Author(s) 2023. CC BY 4.0 License.

The $\delta^2$H peak in spruce bulk stem water was detected after 15 days, and comparable tree water transit times, linked to slow tree water transport velocity, have been observed in different settings, after 12 days in Magh et al. (2020), 14 days in Seeger and Weiler. (2021), and 9–18 days in Nehemy et al. (2022b). Strong depletion of the tree water isotopic signals after the snowmelt event, comparable to both the bulk soil and the lysimeter water isotopic signal present at the time, suggested that the homogenizing effect of snowmelt extends throughout the soil-vegetation continuum in a sub-arctic forest.

## 5 Conclusion

Our "double" irrigation experiment, where the experimental plot was first saturated with an isotopically highly enriched signal, and afterwards flushed by the isotopically depleted snowmelt signal, allowed us to infer infiltration and soil water mixing mechanisms in shallow sub-arctic till soil. We propose a conceptual model with three infiltration stages that are related to the amount of infiltrating water, heterogeneous subsurface flow, and eventually leads to complete soil water displacement. In the first stage, surface microtopography prompts focused infiltration, where most of the flow is happening vertically through an unsaturated macropore network, bypassing the soil matrix and recharging groundwater storage. The second stage is defined by groundwater level rise through the macropore network, gradual filling the macropores, and the establishment of shallow subsurface lateral fluxes and increased horizontal hydrological connectivity in the soil. During the third stage, soil matrix water replenishment occurs under long-lasting saturation and high groundwater table conditions, which promote matrix flow and pore-water exchange.

The massive and short-lasting infiltration event, accompanied by a quick groundwater table rise, produced highly heterogeneous conditions in the soil and negligible effects on the isotopic composition of the soil matrix below a 45 cm depth. However, the snowmelt event was characterized by the progressive flushing of more mobile soil water and subsequent homogenization of the soil matrix. Our results highlight the unique role of snowmelt in soil water replenishment and isotope dynamics. Our findings stress the importance of improving the understanding of present soil water recharge processes. Quantifying soil water dynamics and sources is critical for quantifying future infiltration patterns in high latitude environments that are particularly sensitive to climate change.

## 6 Data availability

Soil water and groundwater isotopic data available at https://etsin.fairdata.fi/dataset/964149fe-7718-4929-95e9-9deb406d96de.

https://doi.org/10.5194/egusphere-2023-884
Preprint. Discussion started: 19 June 2023
© Author(s) 2023. CC BY 4.0 License.

## 7 Author contributions

BK, HM and PA responsible for funding acquisition, study conceptualization and project administration. PA, HM, FM and MS conducted fieldwork, FM responsible for lab work, and all authors were involved in data analysis. FM responsible for data visualization and preparation of the original draft, PA, HM and MS reviewed and edited the draft.

## 9 Competing interests

The authors declare that they have no conflict of interest.

## 10 Acknowledgements

The study was funded by the Kvantum institute, University of Oulu, and supported by Maa- ja Vesitekniikan Tuki ry grant (43562) and the KH Renlund foundation. Pertti Ala-aho was supported by the Academy of Finland grant 316349. Hannu Marttila was supported by Academy of Finland grants (318930, 316014, 347704, 346163, 337523, 316349), Profi 4 Arcl and the National Freshwater Competence Centre (FWCC). Matthias Sprenger thanks the German Hydrological Society (DHG) for the travel support through their DHG Feldstipendium. The authors thank Valtteri, Kashif, Stephanie, Juho, Danny and Päivi for their help with sample collection, and Annalea for her help with the instrumentalization of the experimental plot.

## References

Aguzzoni, A., Engel, M., Zanotelli, D., Penna, D., Comiti, F., and Tagliavini, M. (2022). Water uptake dynamics in apple trees assessed by an isotope labeling approach. Agricultural Water Management, 266, 107572. https://doi.org/10.1016/j.agwat.2022.107572

Ala–Aho, P., Welker, J. M., Bailey, H., Pedersen, S. H., Kopec, B., Klein, E., Mellat, M., Mustonen, K. R., Noor, K., and Marttila, H. (2021a). Arctic Snow Isotope Hydrology: A Comparative Snow-Water Vapor Study. Atmosphere 2021, Vol. 12, Page 150, 12(2), 150. https://doi.org/10.3390/ATMOS12020150

Ala-Aho, P., Autio, A., Bhattacharjee, J., Isokangas, E., Kujala, K., Marttila, H., Menberu, M., Meriö, L. J., Postila, H., Rauhala, A., Ronkanen, A. K., Rossi, P. M., Saari, M., Haghighi, A. T., & Klove, B. (2021b). What conditions favor the influence of seasonally frozen ground on hydrological partitioning? A systematic review. Environmental Research Letters, 16(4), 043008. https://doi.org/10.1088/1748-9326/ABE82C

Appels, W. M., Bogaart, P. W., and van der Zee, S. E. A. T. M. (2011). Influence of spatial variations of microtopography and infiltration on surface runoff and field scale hydrological connectivity. Advances in Water Resources, 34(2), 303–313. https://doi.org/10.1016/J.ADVWATRES.2010.12.003

https://doi.org/10.5194/egusphere-2023-884
Preprint. Discussion started: 19 June 2023
© Author(s) 2023. CC BY 4.0 License.

Aurela, M., Lohila, A., Tuovinen, J. P., Hatakka, J., Penttilä, T., and Laurila, T. (2015). Carbon dioxide and energy flux measurements in four northern-boreal ecosystems at Pallas. Boreal Environment Research, 20(4), 455–473.

Barbeta, A., Burlett, R., Martín–Gómez, P., Fréjaville, B., Devert, N., Wingate, L., Domec, J. C., and Ogée, J. (2022). Evidence for distinct isotopic compositions of sap and tissue water in tree stems: consequences for plant water source identification. New Phytologist, 233(3), 1121–1132. https://doi.org/10.1111/NPH.17857

Beria, H., Larsen, J. R., Ceperley, N. C., Michelon, A., Vennemann, T., and Schaefli, B. (2018). Understanding snow hydrological processes through the lens of stable water isotopes. Wiley Interdisciplinary Reviews: Water, November 2017, e1311. https://doi.org/10.1002/wat2.1311

Berthold, S., Bentley, L. R., and Hayashi, M. (2004). Integrated hydrogeological and geophysical study of depression-focused groundwater recharge in the Canadian prairies. Water Resources Research, 40(6), 6505. https://doi.org/10.1029/2003WR002982

Beven, K., & Germann, P. (2013). Macropores and water flow in soils revisited. Water Resources Research, 49(6), 3071–3092. https://doi.org/10.1002/WRCR.20156

Bintanja, R., and Andry, O. (2017). Towards a rain-dominated Arctic. Nature Climate Change, 7(4), 263–267. https://doi.org/10.1038/nclimate3240

Blume–Werry, G., Wilson, S. D., Kreyling, J., and Milbau, A. (2016). The hidden season: growing season is 50% longer below than above ground along an arctic elevation gradient. New Phytologist, 209(3), 978–986. https://doi.org/10.1111/NPH.13655

Bogner, C., Mirzaei, M., Ruy, S., and Huwe, B. (2013). Microtopography, water storage and flow patterns in a fine-textured soil under agricultural use. Hydrological Processes, 27(12), 1797–1806. https://doi.org/10.1002/HYP.9337

Bowling, D. R., Schulze, E. S., and Hall, S. J. (2017). Revisiting streamside trees that do not use stream water: can the two water worlds hypothesis and snowpack isotopic effects explain a missing water source? Ecohydrology, 10(1), 1–12. https://doi.org/10.1002/eco.1771

Brooks, J. R., Barnard, H. R., Coulombe, R., and McDonnell, J. J. (2010). Ecohydrologic separation of water between trees and streams in a Mediterranean climate. Nature Geoscience, 3(2), 100–104. https://doi.org/10.1038/ngeo722

Brooks, P. D., Chorover, J., Fan, Y., Godsey, S. E., Maxwell, R. M., Mcnamara, J. P., and Tague, C. (2015). Hydrological partitioning in the critical zone: Recent advances and opportunities for developing transferable understanding of water cycle dynamics. 6973–6987. https://doi.org/10.1002/2015WR017039.Received

Cey, E. E., and Rudolph, D. L. (2009). Field study of macropore flow processes using tension infiltration of a dye tracer in partially saturated soils. Hydrological Processes, 23(12), 1768–1779. https://doi.org/10.1002/hyp.7302

Chen, G., Auerswald, K., and Schnyder, H. (2016). 2H and 18O depletion of water close to organic surfaces. Biogeosciences, 13(10), 3175–3186. https://doi.org/10.5194/bg-13-3175-2016

Craig, H. (1961). Isotopic Variations in Meteoric Waters. Science, 133(3465), 1702–1703. https://doi.org/10.1126/SCIENCE.133.3465.1702

Dansgaard, W. (1964). Stable isotopes in precipitation. Tellus, 16(4), 436–468. https://doi.org/10.1111/j.2153-3490.1964.tb00181.x

Darboux, F., Davy, P., Gascuel–Odoux, C., and Huang, C. (2002). Evolution of soil surface roughness and flowpath connectivity in overland flow experiments. Catena, 46(2–3), 125–139. https://doi.org/10.1016/S0341-8162(01)00162-X

Delbart, N., Le Toan, T., Kergoat, L., and Fedotova, V. (2006). Remote sensing of spring phenology in boreal regions: A free of snow-effect method using NOAA-AVHRR and SPOT-VGT data (1982-2004). Remote Sensing of Environment, 101(1), 52–62. https://doi.org/10.1016/j.rse.2005.11.012

Derby, N. E., and Knighton, R. E. (2001). Field-Scale Preferential Transport of Water and Chloride Tracer by Depression-Focused Recharge. Journal of Environmental Quality, 30(1), 194–199. https://doi.org/10.2134/JEQ2001.301194X

Diao, H., Schuler, P., Goldsmith, G. R., Siegwolf, R. T. W., Saurer, M., and Lehmann, M. M. (2022). Technical note: On uncertainties in plant water isotopic composition following extraction by cryogenic vacuum distillation. Hydrology and Earth System Sciences, 26(22), 5835–5847. https://doi.org/10.5194/HESS-26-5835-2022

Dubbert, M., and Werner, C. (2019). Water fluxes mediated by vegetation: emerging isotopic insights at the soil and atmosphere interfaces. New Phytologist, 221(4), 1754–1763. https://doi.org/10.1111/NPH.15547

Etana, A., Larsbo, M., Keller, T., Arvidsson, J., Schjønning, P., Forkman, J., and Jarvis, N. (2013). Persistent subsoil compaction and its effects on preferential flow patterns in a loamy till soil. Geoderma, 192(1), 430–436. https://doi.org/10.1016/J.GEODERMA.2012.08.015

Evans, S. L., Flores, A. N., Heilig, A., Kohn, M. J., Marshall, H. P., and McNamara, J. P. (2016). Isotopic evidence for lateral flow and diffusive transport, but not sublimation, in a sloped seasonal snowpack, Idaho, USA. Geophysical Research Letters, 43(7), 3298–3306. https://doi.org/10.1002/2015GL067605

Fabiani, G., Penna, D., Barbeta, A., and Klaus, J. (2022). Sapwood and heartwood are not isolated compartments: Consequences for isotope ecohydrology. Ecohydrology, 15(8), e2478. https://doi.org/10.1002/ECO.2478

Finkenbiner, C. E., Good, S. P., Renée Brooks, J., Allen, S. T., and Sasidharan, S. (2022). The extent to which soil hydraulics can explain ecohydrological separation. Nature Communications 2022 13:1, 13(1), 1–8. https://doi.org/10.1038/s41467-022-34215-7

Flury, M., Flühler, H., Jury, W. A., & Leuenberger, J. (1994). Susceptibility of soils to preferential flow of water: A field study. Water Resources Research, 30(7), 1945–1954. https://doi.org/10.1029/94WR00871

Foken, T. (2008). Micrometeorology. Micrometeorology, 1–306. https://doi.org/10.1007/978-3-540-74666-9/COVER

Forkel, M., Carvalhais, N., Rödenbeck, C., Keeling, R., Heimann, M., Thonicke, K., Zaehle, S., and Reichstein, M. (2016). Enhanced seasonal CO2 exchange caused by amplified plant productivity in northern ecosystems. Science, 351(6274), 696–699. https://doi.org/10.1126/science.aac4971

https://doi.org/10.5194/egusphere-2023-884
Preprint. Discussion started: 19 June 2023
© Author(s) 2023. CC BY 4.0 License.

Frei, S., Knorr, K. H., Peiffer, S., and Fleckenstein, J. H. (2012). Surface micro-topography causes hot spots of biogeochemical activity in wetland systems: A virtual modeling experiment. Journal of Geophysical Research: Biogeosciences, 117(G4), 0–12. https://doi.org/10.1029/2012JG002012

Frei, S., Lischeid, G., and Fleckenstein, J. H. (2010). Effects of micro-topography on surface–subsurface exchange and runoff generation in a virtual riparian wetland — A modeling study. Advances in Water Resources, 33(11), 1388–1401. https://doi.org/10.1016/J.ADVWATRES.2010.07.006

French, H., and Binley, A. (2004). Snowmelt infiltration: monitoring temporal and spatial variability using time-lapse electrical resistivity. Journal of Hydrology, 297(1–4), 174–186. https://doi.org/10.1016/J.JHYDROL.2004.04.005

Goldsmith, G. R., Allen, S. T., Braun, S., Engbersen, N., González-Quijano, C. R., Kirchner, J. W., and Siegwolf, R. T. W. (2019). Spatial variation in throughfall, soil, and plant water isotopes in a temperate forest. Ecohydrology, 12(2), e2059. https://doi.org/10.1002/ECO.2059

Gonfiantini, R. (1978). Standards for stable isotope measurements in natural compounds. Nature 1978 271:5645, 271(5645), 534–536. https://doi.org/10.1038/271534a0

Good, S. P., Noone, D., and Bowen, G. (2015). Hydrologic connectivity constrains partitioning of global terrestrial water fluxes. Science, 349(6244), 175–177. https://doi.org/10.1126/science.aaa5931

Groisman, P. Y., Karl, T. R., and Knight, R. W. (1994). Observed impact of snow cover on the heat balance and the rise of continental spring temperatures. Science, 263(5144), 198–200. https://doi.org/10.1126/science.263.5144.198

Hansen, B. (2000). Estimation of surface runoff and water-covered area during filling of surface microrelief depressions. Hydrological Processes, 14(7), 1235–1243. https://doi.org/10.1002/(SICI)1099-1085(200005)14:7<1235::AID-HYP38>3.0.CO;2-W

Hassol, S. J. (2004). Impacts of a Warming Arctic - Arctic Climate Impact Assessment. In iwaa. Cambridge University Press. https://ui.adsabs.harvard.edu/abs/2004iwaa.book.....A/abstract

Hatami, S., and Nazemi, A. (2022). Compound changes in temperature and snow depth lead to asymmetric and nonlinear responses in landscape freeze–thaw. Scientific Reports, 12(1), 1–13. https://doi.org/10.1038/s41598-022-06320-6

Hayashi, M. (2013). The Cold Vadose Zone: Hydrological and Ecological Significance of Frozen-Soil Processes. Vadose Zone Journal, 12(4), 1–8. https://doi.org/10.2136/VZJ2013.03.0064

Hayashi, M., Van Der Kamp, G., and Schmidt, R. (2003). Focused infiltration of snowmelt water in partially frozen soil under small depressions. Journal of Hydrology, 270(3–4), 214–229. https://doi.org/10.1016/S0022-1694(02)00287-1

Henry, H. A. L. (2008). Climate change and soil freezing dynamics: Historical trends and projected changes. Climatic Change, 87(3–4), 421–434. https://doi.org/10.1007/s10584-007-9322-8

Hölttä, T., Dominguez Carrasco, M. D. R., Salmon, Y., Aalto, J., Vanhatalo, A., Bäck, J., and Lintunen, A. (2018). Water relations in silver birch during springtime: How is sap pressurised? Plant Biology, 20(5), 834–847. https://doi.org/10.1111/PLB.12838

https://doi.org/10.5194/egusphere-2023-884
Preprint. Discussion started: 19 June 2023
© Author(s) 2023. CC BY 4.0 License.

Hrachowitz, M., Savenije, H., Bogaard, T. A., Tetzlaff, D., and Soulsby, C. (2013). What can flux tracking teach us about water age distribution patterns and their temporal dynamics? Hydrology and Earth System Sciences, 17(2), 533–564. https://doi.org/10.5194/HESS-17-533-2013

Hutson, J. L., and Wagenet, R. J. (1995). A Multiregion Model Describing Water Flow and Solute Transport in Heterogeneous Soils. Soil Science Society of America Journal, 59(3), 743–751. https://doi.org/10.2136/SSSAJ1995.03615995005900030016X

Hyman–Rabeler, K. A., and Loheide, S. P. (2023). Drivers of Variation in Winter and Spring Groundwater Recharge: Impacts of Midwinter Melt Events and Subsequent Freezeback. Water Resources Research, 59(1), e2022WR032733. https://doi.org/10.1029/2022WR032733

Ireson, A. M., van der Kamp, G., Ferguson, G., Nachshon, U., and Wheater, H. S. (2013). Hydrogeological processes in seasonally frozen northern latitudes: understanding, gaps and challenges. Hydrogeology Journal, 21(1), 53–66. https://doi.org/10.1007/s10040-012-0916-5

Jarvis, N. J. (2007). A review of non-equilibrium water flow and solute transport in soil macropores: Principles, controlling factors and consequences for water quality. In European Journal of Soil Science (Vol. 58, Issue 3, pp. 523–546). John Wiley and Sons, Ltd. https://doi.org/10.1111/j.1365-2389.2007.00915.x

Jeong, S. J., Ho, C. H., Gim, H. J., and Brown, M. E. (2011). Phenology shifts at start vs. end of growing season in temperate vegetation over the Northern Hemisphere for the period 1982-2008. Global Change Biology, 17(7), 2385–2399. https://doi.org/10.1111/j.1365-2486.2011.02397.x

Johansson, P., Lunkka, J. P., and Sarala, P. (2011). The Glaciation of Finland. Developments in Quaternary Science, 15, 105–116. https://doi.org/10.1016/B978-0-444-53447-7.00009-X

Kampf, S., Markus, J., Heath, J., and Moore, C. (2015). Snowmelt runoff and soil moisture dynamics on steep subalpine hillslopes. Hydrological Processes, 29(5), 712–723. https://doi.org/10.1002/HYP.10179

Kendall, K. A., Shanley, J. B., and McDonnell, J. J. (1999). A hydrometric and geochemical approach to test the transmissivity feedback hypothesis during snowmelt. Journal of Hydrology, 219(3–4), 188–205. https://doi.org/10.1016/S0022-1694(99)00059-1

Klaus, J., Zehe, E., Elsner, M., Külls, C., & McDonnell, J. J. (2013). Macropore flow of old water revisited: Experimental insights from a tile-drained hillslope. Hydrology and Earth System Sciences, 17(1), 103–118. https://doi.org/10.5194/hess-17-103-2013

Klein Tank, A., Rusticucci, M., Alexander, L., Brönnimann, S., Charabi, Y., Dentener, F., Dlugokencky, E., Easterling, D., Kaplan, A., Soden, B., Thorne, P., Wild, M., Zhai, P., Qin, D., Plattner, G., Tignor, M., Allen, S., Boschung, J., Nauels, A., … Blake, D. (2013). Observations: Atmosphere and Surface. In: Climate Change 2013: The Physical Science Basis. Contribution of Working Group I to the Fifth Assessment Report of the Intergovernmental Panel on Climate Change Coordinating Lead Authors: Lead Authors: Contributing Authors.

© Author(s) 2023. CC BY 4.0 License.

Korkiakoski, M., Määttä, T., Peltoniemi, K., Penttilä, T., and Lohila, A. (2022). Excess soil moisture and fresh carbon input are prerequisites for methane production in podzolic soil. Biogeosciences, 19(7), 2025–2041. https://doi.org/10.5194/BG-19-2025-2022

Kulli, B., Gysi, M., and Flühler, H. (2003). Visualizing soil compaction based on flow pattern analysis. Soil and Tillage Research, 70(1), 29–40. https://doi.org/10.1016/S0167-1987(02)00121-6

Larsbo, M., and Jarvis, N. (2005). Simulating Solute Transport in a Structured Field Soil: Uncertainty in Parameter Identification and Predictions. Journal of Environmental Quality, 34(2), 621–634. https://doi.org/10.2134/JEQ2005.0621

Laudon, H., Seibert, J., Köhler, S., and Bishop, K. (2004). Hydrological flow paths during snowmelt: Congruence between hydrometric measurements and oxygen 18 in meltwater, soil water, and runoff. Water Resources Research, 40(3), 3102. https://doi.org/10.1029/2003WR002455

Laudon, H., Spence, C., Buttle, J., Carey, S. K., McDonnell, J. J., McNamara, J. P., Soulsby, C., and Tetzlaff, D. (2017). Save northern high-latitude catchments. Nature Geoscience, 10(5), 324–325. https://doi.org/10.1038/ngeo2947

Li, X.-Y., Ma, Y.-J., Zhang, Z.-H., Peng, H.-Y., Zhang, S.-Y., Li, G.-Y., Li, L., Zone, V., Li, X.-Y., Hu, X., Zhang, Z.-H., Peng, H.-Y., Zhang, S.-Y., Li, G.-Y., Li, L., and Ma, Y.-J. (2013). Shrub Hydropedology: Preferential Water Availability to Deep Soil Layer. Vadose Zone Journal, 12(4), 1–12. https://doi.org/10.2136/VZJ2013.01.0006

Liu, H., and Lin, H. (2015). Frequency and Control of Subsurface Preferential Flow: From Pedon to Catchment Scales. Soil Science Society of America Journal, 79(2), 362–377. https://doi.org/10.2136/SSSAJ2014.08.0330

Lohila, A., Penttiliä, T., Jortikka, S., Aalto, T., Anttila, P., Asmi, E., Aurela, M., Hatakka, J., Hellén, H., Henttonen, H., Hänninen, P., Kilkki, J., Kyllönen, K., Laurila, T., Lepistö, A., Lihavainen, H., Makkonen, U., Paatero, J., Rask, M., and Sutinen, R. (2015). Preface to the special issue on integrated research of atmosphere, ecosystem and environment at Pallas. Boreal Environment Research, 20(4), 431–454.

Luo, L., Lin, H., and Halleck, P. (2008). Quantifying Soil Structure and Preferential Flow in Intact Soil Using X-ray Computed Tomography. Soil Science Society of America Journal, 72(4), 1058–1069. https://doi.org/10.2136/SSSAJ2007.0179

Ma, Y. jun, Li, X. yan, Guo, L., and Lin, H. (2017). Hydropedology: Interactions between pedologic and hydrologic processes across spatiotemporal scales. Earth-Science Reviews, 171(19), 181–195. https://doi.org/10.1016/j.earscirev.2017.05.014

Magh, R. K., Eiferle, C., Burzlaff, T., Dannenmann, M., Rennenberg, H., and Dubbert, M. (2020). Competition for water rather than facilitation in mixed beech-fir forests after drying-wetting cycle. Journal of Hydrology, 587, 124944. https://doi.org/10.1016/j.jhydrol.2020.124944

Manning, G., Fuller, L. G., Eilers, R. G., and Florinsky, I. (2001). Topographic influence on the variability of soil properties within an undulating Manitoba landscape. Canadian Journal of Soil Science, 81(4), 439–447. https://doi.org/10.4141/S00-057

https://doi.org/10.5194/egusphere-2023-884
Preprint. Discussion started: 19 June 2023
© Author(s) 2023. CC BY 4.0 License.

Martín–Gómez, P., Barbeta, A., Voltas, J., Peñuelas, J., Dennis, K., Palacio, S., Dawson, T. E., and Ferrio, J. P. (2015). Isotope-ratio infrared spectroscopy: A reliable tool for the investigation of plant-water sources? New Phytologist, 207(3), 914–927. https://doi.org/10.1111/NPH.13376

Marttila, H., Lohila, A., Ala–Aho, P., Noor, K., Welker, J. M., Croghan, D., Mustonen, K., Meriö, L. J., Autio, A., Muhic, F., Bailey, H., Aurela, M., Vuorenmaa, J., Penttilä, T., Hyöky, V., Klein, E., Kuzmin, A., Korpelainen, P., Kumpula, T., … Kløve, B. (2021). Subarctic catchment water storage and carbon cycling – Leading the way for future studies using integrated datasets at Pallas, Finland. Hydrological Processes, 35(9), e14350. https://doi.org/10.1002/HYP.14350

McDonnell, J. J. (1990). A Rationale for Old Water Discharge Through Macropores in a Steep, Humid Catchment. Water Resources Research, 26(11), 2821–2832. https://doi.org/10.1029/WR026I011P02821

McDonnell, J. J. (2014). The two water worlds hypothesis: ecohydrological separation of water between streams and trees? Wiley Interdisciplinary Reviews: Water, n/a-n/a. https://doi.org/10.1002/wat2.1027

Michelon, A., Ceperley, N., Beria, H., Larsen, J., Vennemann, T., and Schaefli, B. (2023). Hydrodynamics of a high Alpine catchment characterized by four natural tracers. Hydrology and Earth System Sciences, 27(7), 1403–1430. https://doi.org/10.5194/HESS-27-1403-2023

Millar, C., Pratt, D., Schneider, D. J., and McDonnell, J. J. (2018). A comparison of extraction systems for plant water stable isotope analysis. Rapid Communications in Mass Spectrometry, 32(13), 1031–1044. https://doi.org/10.1002/RCM.8136

Mioduszewski, J. R., Rennermalm, A. K., Robinson, D. A., and Mote, T. L. (2014). Attribution of snowmelt onset in Northern Canada. Journal of Geophysical Research: Atmospheres, 119(16), 9638–9653. https://doi.org/10.1002/2013JD021024

Mohammed, A. A., Kurylyk, B. L., Cey, E. E., & Hayashi, M. (2018). Snowmelt Infiltration and Macropore Flow in Frozen Soils: Overview, Knowledge Gaps, and a Conceptual Framework. Vadose Zone Journal, 17(1), 1–15. https://doi.org/10.2136/VZJ2018.04.0084

Mueller, M. H., Alaoui, A., Kuells, C., Leistert, H., Meusburger, K., Stumpp, C., Weiler, M., and Alewell, C. (2014). Tracking water pathways in steep hillslopes by δ18O depth profiles of soil water. Journal of Hydrology, 519(PA), 340–352. https://doi.org/10.1016/j.jhydrol.2014.07.031

Muhic, F., Ala-Aho, P., Noor, K., Welker, J. M., Klöve, B., and Marttila, H. (2023). Flushing or mixing? Stable water isotopes reveal differences in arctic forest and peatland soil water seasonality. Hydrological Processes, 37(1), e14811. https://doi.org/10.1002/hyp.14811

Nehemy, M. F., Benettin, P., Allen, S. T., Steppe, K., Rinaldo, A., Lehmann, M. M., and McDonnell, J. J. (2022a). Phloem water isotopically different to xylem water: Potential causes and implications for ecohydrological tracing. Ecohydrology. https://doi.org/10.1002/ECO.2417

© Author(s) 2023. CC BY 4.0 License.

Nehemy, M. F., Maillet, J., Perron, N., Pappas, C., Sonnentag, O., Baltzer, J. L., Laroque, C. P., and McDonnell, J. J. (2022b). Snowmelt Water Use at Transpiration Onset: Phenology, Isotope Tracing, and Tree Water Transit Time. Water Resources Research, 58(9), e2022WR032344. https://doi.org/10.1029/2022WR032344

Newman, B. D., Wilcox, B. P., & Graham, R. C. (2004). Snowmelt-driven macropore flow and soil saturation in a semiarid forest. Hydrological Processes, 18(5), 1035–1042. https://doi.org/10.1002/HYP.5521

Noor, K., Marttila, H., Klöve, B., Welker, J. M., and Ala–aho, P. (2023). The Spatiotemporal Variability of Snowpack and Snowmelt Water 18O and 2H Isotopes in a Subarctic Catchment. Water Resources Research, 59(1), e2022WR033101. https://doi.org/10.1029/2022WR033101

Oshun, J., Dietrich, W. E., Dawson, T. E., and Fung, I. (2016). Dynamic, structured heterogeneity of water isotopes inside hillslopes. Water Resources Research, 52(1), 164–189. https://doi.org/10.1002/2015WR017485

Pau, S., Wolkovich, E. M., Cook, B. I., Davies, T. J., Kraft, N. J. B., Bolmgren, K., Betancourt, J. L., and Cleland, E. E. (2011). Predicting phenology by integrating ecology, evolution and climate science. In Global Change Biology (Vol. 17, Issue 12, pp. 3633–3643). John Wiley and Sons, Ltd. https://doi.org/10.1111/j.1365-2486.2011.02515.x

Penna, D., Borga, M., Norbiato, D., and Dalla Fontana, G. (2009). Hillslope scale soil moisture variability in a steep alpine terrain. Journal of Hydrology, 364(3–4), 311–327. https://doi.org/10.1016/J.JHYDROL.2008.11.009

Post, E., Forchhammer, M. C., Bret–Harte, M. S., Callaghan, T. V., Christensen, T. R., Elberling, B., Fox, A. D., Gilg, O., Hik, D. S., Høye, T. T., Ims, R. A., Jeppesen, E., Klein, D. R., Madsen, J., McGuire, A. D., Rysgaard, S., Schindler, D. E., Stirling, I., Tamstorf, M. P., … Aastrup, P. (2009). Ecological dynamics across the arctic associated with recent climate change. In Science (Vol. 325, Issue 5946, pp. 1355–1358). American Association for the Advancement of Science. https://doi.org/10.1126/science.1173113

Pulliainen, J., Luojus, K., Derksen, C., Mudryk, L., Lemmetyinen, J., Salminen, M., Ikonen, J., Takala, M., Cohen, J., Smolander, T., and Norberg, J. (2020). Patterns and trends of Northern Hemisphere snow mass from 1980 to 2018. Nature, 581(7808), 294–298. https://doi.org/10.1038/S41586-020-2258-0

Rothfuss, Y., Merz, S., Vanderborght, J., Hermes, N., Weuthen, A., Pohlmeier, A., Vereecken, H., and Brüggemann, N. (2015). Long-term and high-frequency non-destructive monitoring of water stable isotope profiles in an evaporating soil column. Hydrology and Earth System Sciences, 19(10), 4067–4080. https://doi.org/10.5194/HESS-19-4067-2015

Rouxel, M., Molénat, J., Ruiz, L., Legout, C., Faucheux, M., and Gascuel-Odoux, C. (2011). Seasonal and spatial variation in groundwater quality along the hillslope of an agricultural research catchment (Western France). Hydrological Processes, 25(6), 831–841. https://doi.org/10.1002/HYP.7862

Rozanski, K., Araguás–Araguás, L., and Gonfiantini, R. (2013). Isotopic Patterns in Modern Global Precipitation. In Climate Change in Continental Isotopic Records Geophysical Monograph (Vol. 78, pp. 1–36). https://doi.org/10.1029/gm078p0001

Scherrer, S., Naef, F., Fach, A. O., and Cordery, I. (2007). Formation of runoff at the hillslope scale during intense precipitation. Hydrology and Earth System Sciences, 11(2), 907–922. https://doi.org/10.5194/hess-11-907-2007

Schlüter, S., Vanderborght, J., and Vogel, H. J. (2012). Hydraulic non-equilibrium during infiltration induced by structural connectivity. Advances in Water Resources, 44, 101–112. https://doi.org/10.1016/J.ADVWATRES.2012.05.002

Seeger, S., and Weiler, M. (2021). Temporal dynamics of tree xylem water isotopes: In situ monitoring and modeling. Biogeosciences, 18(15), 4603–4627. https://doi.org/10.5194/bg-18-4603-2021

Seeger, S., and Weiler, M. (2023). Dye tracer aided investigation of xylem water transport velocity distributions. January. https://doi.org/10.5194/egusphere-2022-1492

Shen, M., Tang, Y., Chen, J., Yang, X., Wang, C., Cui, X., Yang, Y., Han, L., Li, L., Du, J., Zhang, G., and Cong, N. (2014). Earlier-Season Vegetation Has Greater Temperature Sensitivity of Spring Phenology in Northern Hemisphere. PLOS ONE, 9(2), e88178. https://doi.org/10.1371/JOURNAL.PONE.0088178

Šimůnek, J., Jarvis, N. J., Van Genuchten, M. T., and Gärdenäs, A. (2003). Review and comparison of models for describing non-equilibrium and preferential flow and transport in the vadose zone. Journal of Hydrology, 272(1–4), 14–35. https://doi.org/10.1016/S0022-1694(02)00252-4

Smith, T. J., Mcnamara, J. P., Flores, A. N., Gribb, M. M., Aishlin, P. S., and Benner, S. G. (2011). Small soil storage capacity limits benefit of winter snowpack to upland vegetation. Hydrological Processes, 25(25), 3858–3865. https://doi.org/10.1002/HYP.8340

Sněhota, M., Císlerová, M., Amin, M. H. G., and Hall, L. D. (2010). Tracing the Entrapped Air in Heterogeneous Soil by Means of Magnetic Resonance Imaging. Vadose Zone Journal, 9(2), 373–384. https://doi.org/10.2136/VZJ2009.0103

Sprenger, M., and Allen, S. T. (2020). What Ecohydrologic Separation Is and Where We Can Go With It. Water Resources Research, 56(7), e2020WR027238. https://doi.org/10.1029/2020WR027238

Sprenger, M., Leistert, H., Gimbel, K., and Weiler, M. (2016). Illuminating hydrological processes at the soil-vegetation-atmosphere interface with water stable isotopes. Reviews of Geophysics, 54(3), 674–704. https://doi.org/10.1002/2015RG000515

Sprenger, M., Llorens, P., Cayuela, C., Gallart, F., and Latron, J. (2019). Mechanisms of consistently disjunct soil water pools over (pore) space and time. Hydrology and Earth System Sciences, 23(6), 2751–2762. https://doi.org/10.5194/HESS-23-2751-2019

Sprenger, M., Tetzlaff, D., Buttle, J., Laudon, H., Leistert, H., Mitchell, C. P. J., Snelgrove, J., Weiler, M., and Soulsby, C. (2018a). Measuring and Modeling Stable Isotopes of Mobile and Bulk Soil Water. Vadose Zone Journal, 17(1), 1–18. https://doi.org/10.2136/VZJ2017.08.0149

Sprenger, M., Tetzlaff, D., Buttle, J., Laudon, H., and Soulsby, C. (2018b). Water ages in the critical zone of long-term experimental sites in northern latitudes. Hydrol. Earth Syst. Sci, 22, 3965–3981. https://doi.org/10.5194/hess-22-3965-2018

Sprenger, M., Tetzlaff, D., and Soulsby, C. (2017). Soil water stable isotopes reveal evaporation dynamics at the soil-plant-atmosphere interface of the critical zone. Hydrology and Earth System Sciences, 21(7), 3839–3856. https://doi.org/10.5194/hess-21-3839-2017

© Author(s) 2023. CC BY 4.0 License.

Stiegler, C., Lund, M., Røjle Christensen, T., Mastepanov, M., and Lindroth, A. (2016). Two years with extreme and little snowfall: Effects on energy partitioning and surface energy exchange in a high-Arctic tundra ecosystem. Cryosphere, 10(4), 1395–1413. https://doi.org/10.5194/tc-10-1395-2016

Stumpp, C., and Hendry, M. J. (2012). Spatial and temporal dynamics of water flow and solute transport in a heterogeneous glacial till: The application of high-resolution profiles of δ18O and δ2H in pore waters. Journal of Hydrology, 438–439, 203–214. https://doi.org/10.1016/J.JHYDROL.2012.03.024

Sutinen, R., Äikää, O., Piekkari, M., and Hänninen, P. (2009). Snowmelt infiltration through partially frozen soil in Finnish Lapland. Geophysica, 45(1–2), 27–39.

Sutinen, R., Vajda, A., Hänninen, P., and Sutinen, M. –L. (2009). Significance of Snowpack for Root-zone Water and Temperature Cycles in Subarctic Lapland. Arctic, Antarctic, and Alpine Research, 41(3), 373–380. https://doi.org/10.1657/1938-4246-41.3.373

Tetzlaff, D., Buttle, J., Carey, S. K., Mcguire, K., Laudon, H., and Soulsby, C. (2015). Tracer-based assessment of flow paths, storage and runoff generation in northern catchments: A review. Hydrological Processes, 29(16), 3475–3490. https://doi.org/10.1002/hyp.10412

Treydte, K., Lehmann, M. M., Wyczesany, T., and Pfautsch, S. (2021). Radial and axial water movement in adult trees recorded by stable isotope tracing. Tree Physiology, 41(12), 2248–2261. https://doi.org/10.1093/TREEPHYS/TPAB080

Tromp–Van Meerveld, H. J., and McDonnell, J. J. (2006). Threshold relations in subsurface stormflow: 2. The fill and spill hypothesis. Water Resources Research, 42(2), 2411. https://doi.org/10.1029/2004WR003800

Vaganov, E. A., Hughes, M. K., Kirdyanov, A. V., Schweingruber, F. H., and Silkin, P. P. (1999). Influence of snowfall and melt timing on tree growth in subarctic Eurasia. Nature, 400(6740), 149–151. https://doi.org/10.1038/22087

van Genuchten, M. T. (1980). A Closed-form Equation for Predicting the Hydraulic Conductivity of Unsaturated Soils. Soil Science Society of America Journal, 44(5), 892–898. https://doi.org/10.2136/sssaj1980.03615995004400050002x

Vereecken, H., Huisman, J. A., Hendricks Franssen, H. J., Brüggemann, N., Bogena, H. R., Kollet, S., Javaux, M., Van Der Kruk, J., and Vanderborght, J. (2015). Soil hydrology: Recent methodological advances, challenges, and perspectives. Water Resources Research, 51(4), 2616–2633. https://doi.org/10.1002/2014WR016852

Wassenaar, L. I., Hendry, M. J., Chostner, V. L., and Lis, G. P. (2008). High resolution pore water δ2H and δ18O measurements by H2O(liquid)-H2O (vapor) equilibration laser spectroscopy. Environmental Science and Technology, 42(24), 9262–9267. https://doi.org/10.1021/es802065s

Weiler, M. (2005). An infiltration model based on flow variability in macropores: development, sensitivity analysis and applications. Journal of Hydrology, 310(1–4), 294–315. https://doi.org/10.1016/J.JHYDROL.2005.01.010

Weiler, M., & Naef, F. (2003). An experimental tracer study of the role of macropores in infiltration in grassland soils. Hydrological Processes, 17(2), 477–493. https://doi.org/10.1002/HYP.1136

https://doi.org/10.5194/egusphere-2023-884
Preprint. Discussion started: 19 June 2023
© Author(s) 2023. CC BY 4.0 License.

West, A. G., Patrickson, S. J., and Ehleringer, J. R. (2006). Water extraction times for plant and soil materials used in stable isotope analysis. Rapid Communications in Mass Spectrometry, 20(8), 1317–1321. https://doi.org/10.1002/RCM.2456

Xiao, X., Zhang, F., Li, X., Wang, G., Zeng, C., and Shi, X. (2020). Hydrological functioning of thawing soil water in a permafrost-influenced alpine meadow hillslope. Vadose Zone Journal, 19(1), e20022. https://doi.org/10.1002/VZJ2.20022